Tayler-Spruit dynamo, low-field magnetars and central compact objects

Andrei P. Igoshev
Rainer Hollerbach, Toby Wood,
Jerome Guilet,
Raphael Raynoud, Paul Barrere
Nicolas Moraga

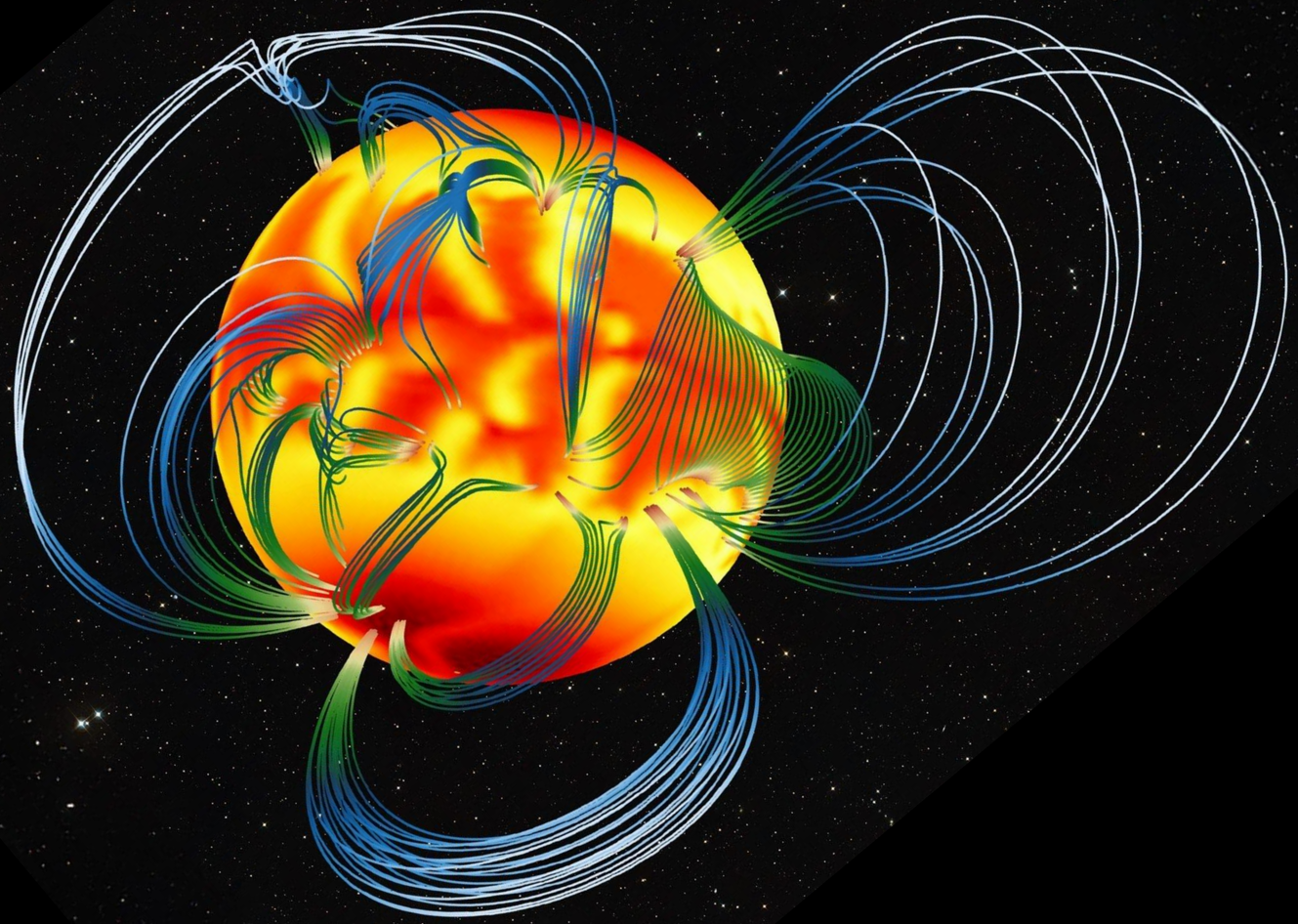

THE ROYAL SOCIETY

24/06/2026

Research group at Newcastle University, UK

Superconductivity in neutron star cores

Main objective: to model magnetic field evolution in superconducting neutron stars cores

Recent side project: hydrodynamic model for pulsar glitches

Dr Nicolas Moraga

Charlie Perkins

Thursday 17:30

Neutron stars & their magnetic fields

- Neutron stars (NSs) are compact (~10 km) remnants of the stellar evolution. A mass of NS is $\approx 1.4 M_{\odot}$. NSs have extreme magnetic fields ($10^{8} - 10^{14}$ G).
- Main observational characteristics for neutron stars are their period and period derivatives.
- P and $\dot{P}$ indicate poloidal, dipolar magnetic field strength B_p

$$B \propto \sqrt{P\dot{P}}$$

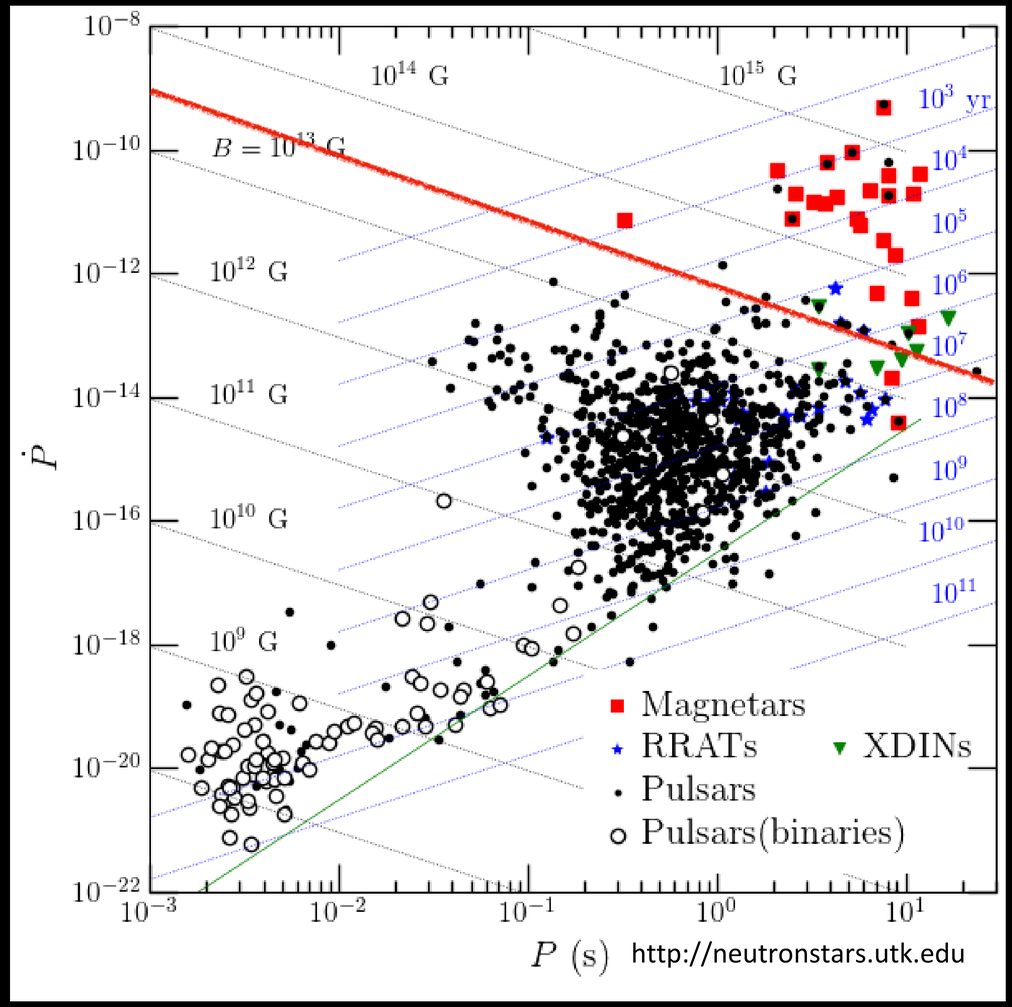

Review on magnetic field evolution: Igoshev, Popov & Hollerbach (2021)
Review on techniques: Pons, Dehman & Vigano (2026)

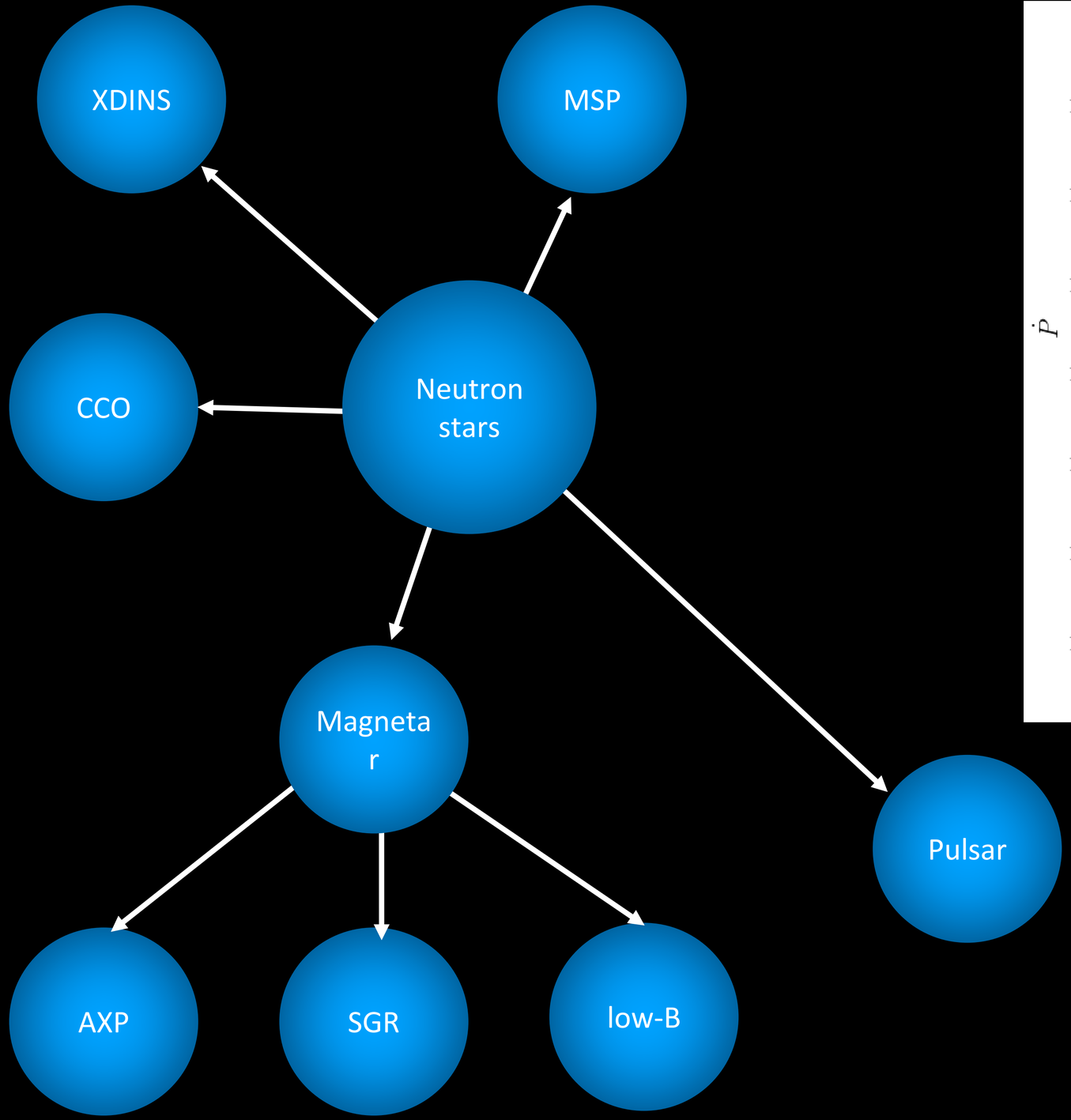

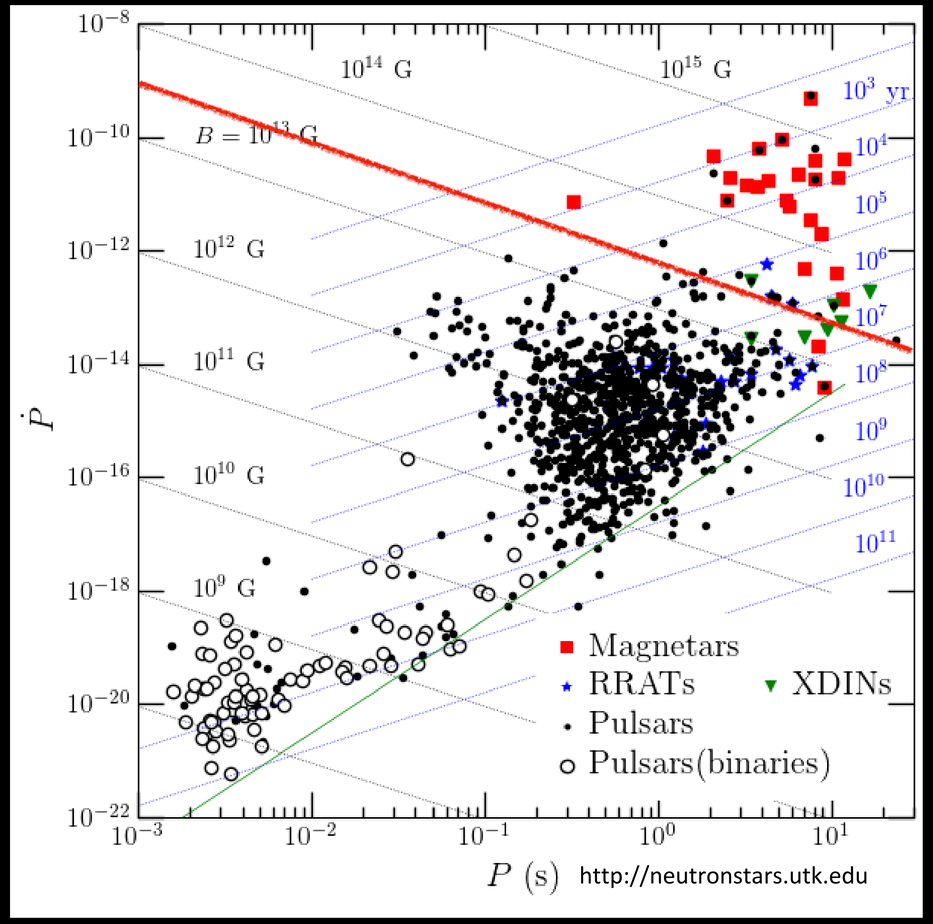

NS zoo,
Harding (2013);
Borghese (2024)

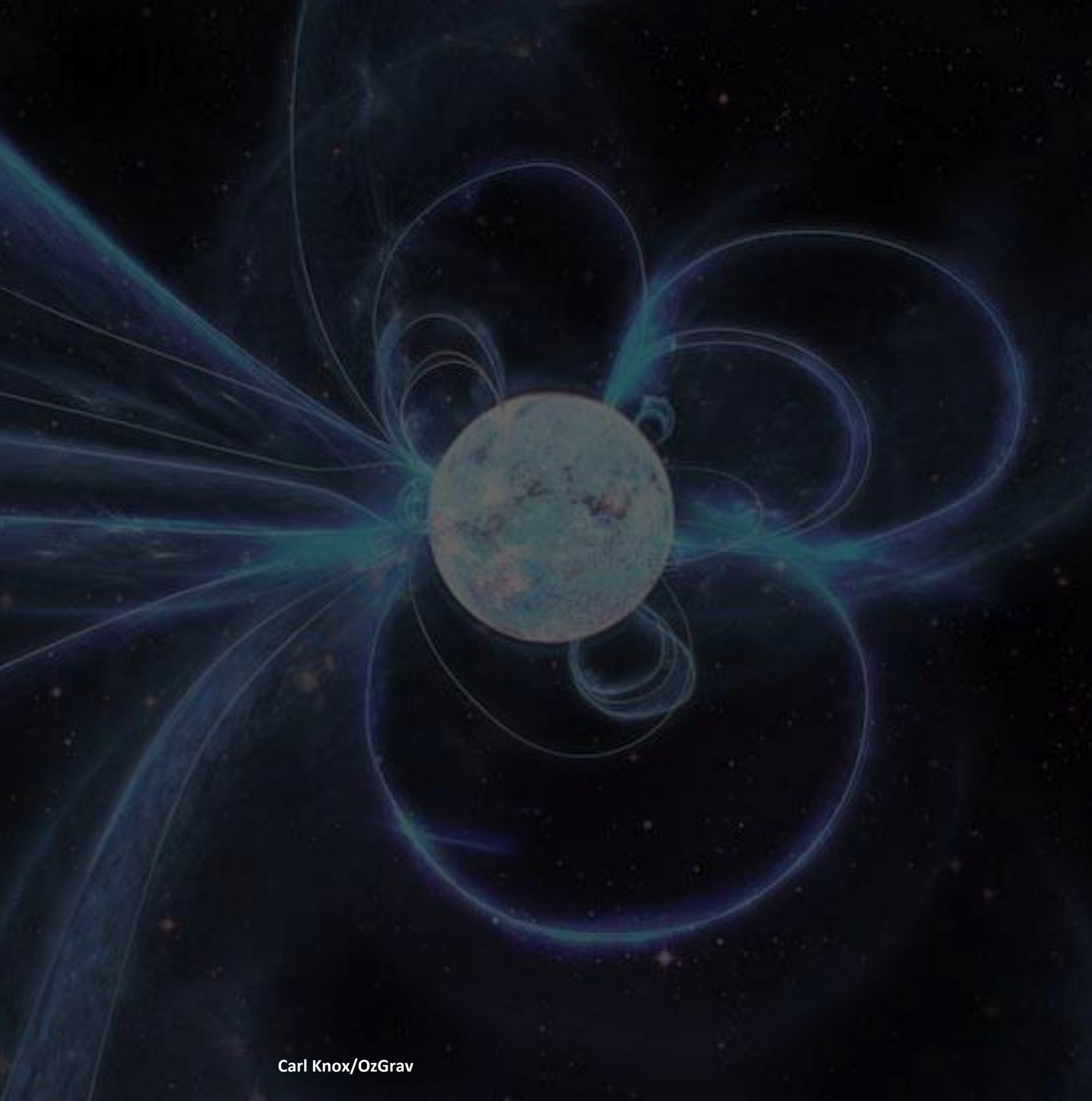

Magnetars

Two classes of neutron stars: **Anomalous X-ray Pulsars** (AXP) and **Soft Gamma Repeaters** (SGR) are combined as magnetars.

Anomalous X-ray pulsars emit thermal X-ray modulating with rotational phase. No obvious sources of accretions are detected: AXPs are isolated.

Soft Gamma Repeaters emit large burst of X-rays and gamma rays episodically. Large emission episodes show modulation with a period of a NS.

Low-B magnetars have burst and outbursts but their dipolar magnetic fields are weaker than 4×10^{13} G

Carl Knox/OzGrav

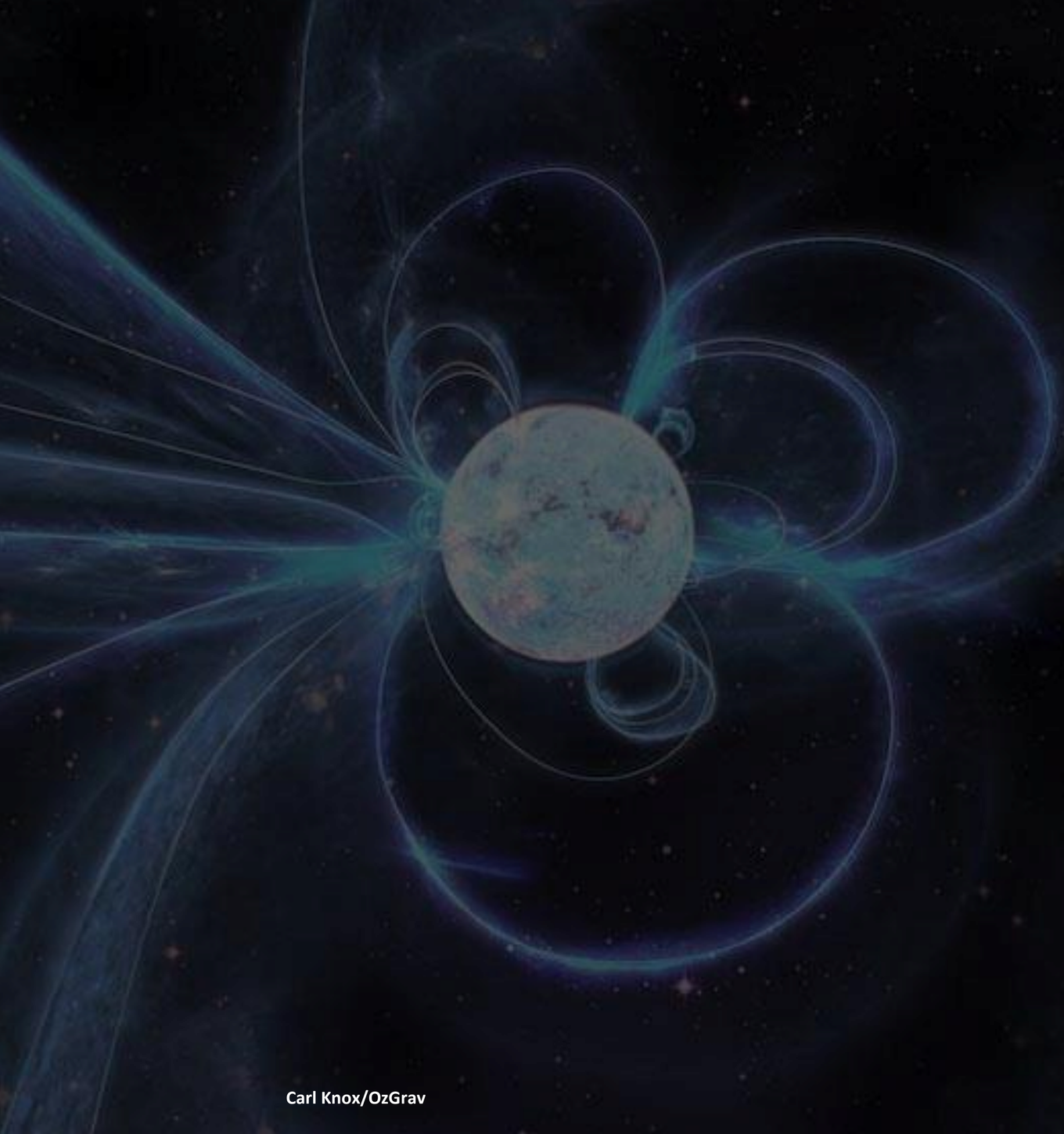

Magnetars

Magnetars are defined now based on their transient behaviour i.e. as sources with burst and outbursts in X-ray.

Carl Knox/OzGrav

XDINS and their tangled magnetic fields

X-ray spectra is well described with thermal blackbody but in some cases absorption features are present.
Some of these objects have phase dependant absorption features which could be produced by proton cyclotron resonant scattering in a localised loop near NS surface with magnetic field ~5 times stronger than dipolar estimate. Similar is found for low-B magnetars

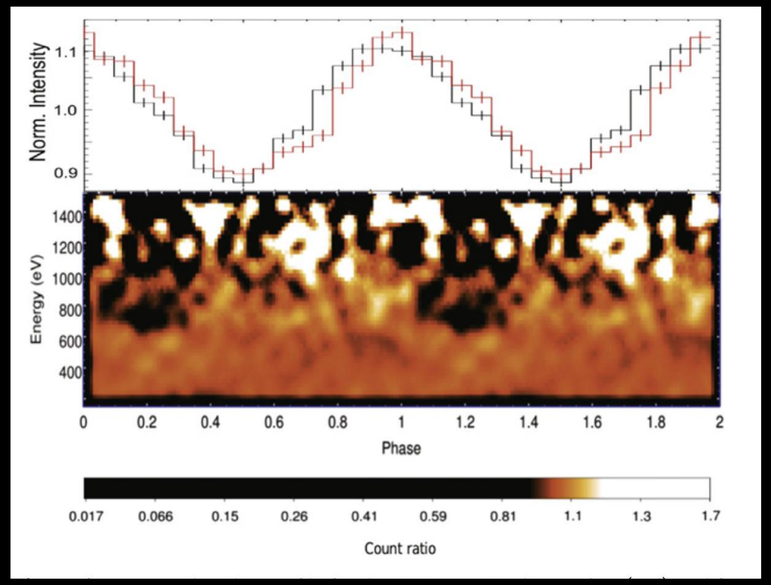

RX J0720.4–3125; Borghese+ (2015)

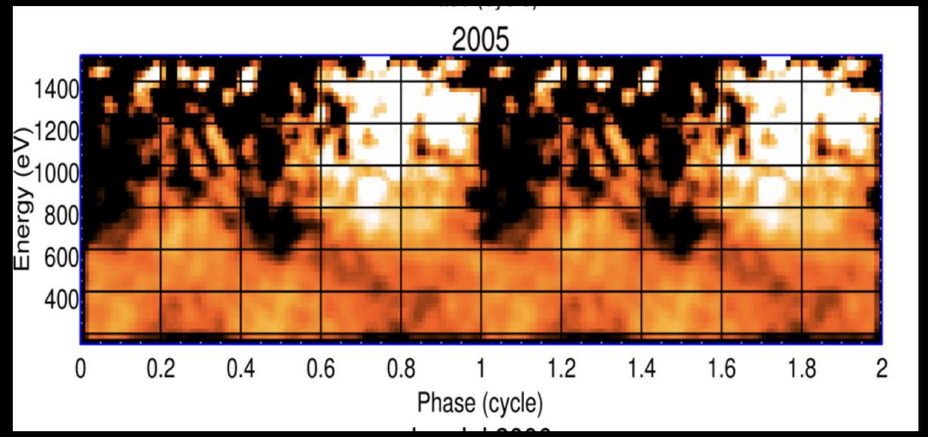

RX J1308.6+21275; Borghese+ (2017)

XDINS and their tangled magnetic fields

X-ray spectra is well described with thermal blackbody but in some cases absorption features are present.
Some of these objects have phase dependant absorption features which could be produced by proton cyclotron resonant scattering in a localised loop near NS surface with magnetic field ~5 times stronger than dipolar estimate. Similar is found for low-B magnetars

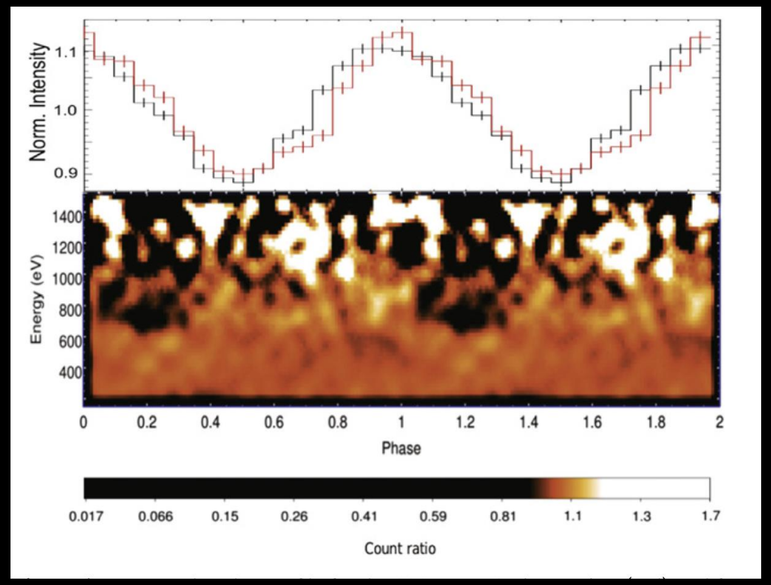

RX J0720.4–3125; Borghese+ (2015)

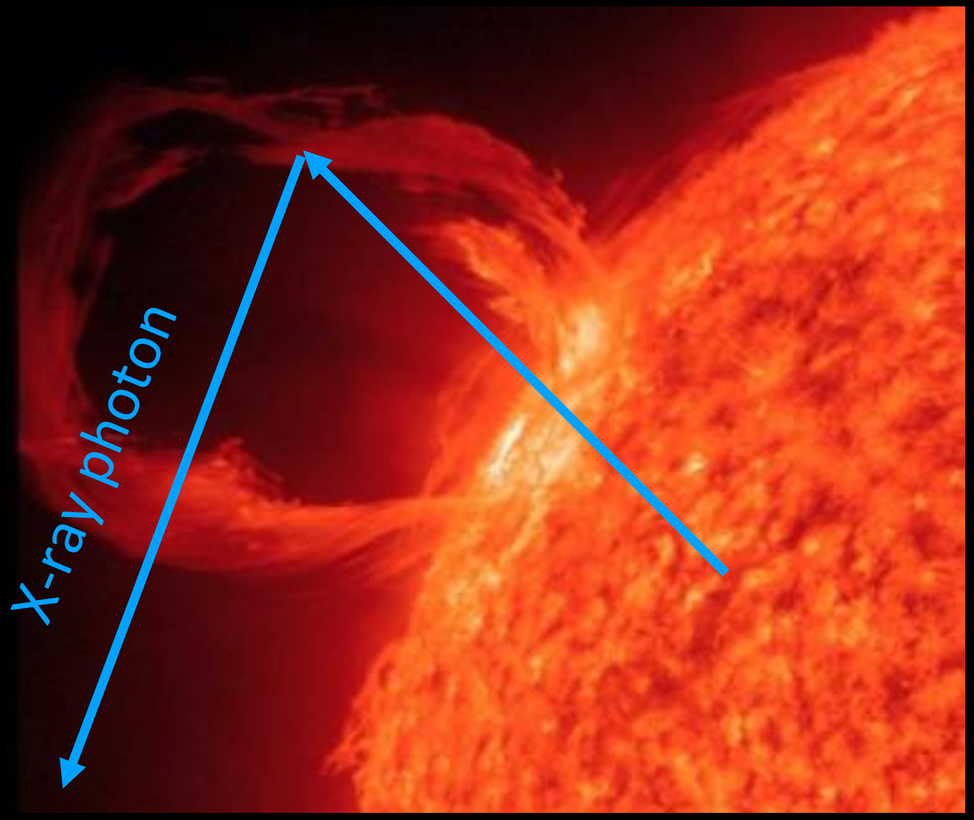

Central compact objects (CCOs)

A handful of young isolated NSs discovered in close vicinity to geometric centra of supernova remnants. (de Luca 2017)

CCOs emit only thermal X-ray radiation. No radio emission was discovered.

Periods and period derivatives are measured in three cases. Periods are typical for normal radio pulsars. Period derivatives are very small ~10^{-17} s/s.

Central compact objects (CCOs)

PF ~ 9-11% in two cases, 64% in one case

Thermal emission of CCOs is stronger than expected based on isolated NS cooling:

$L_{\rm bol}/\dot{E} > 10$

CCO have hidden magnetic fields Hidden = multipolar or toroidal magnetic fields which cannot be measured though spin-down.

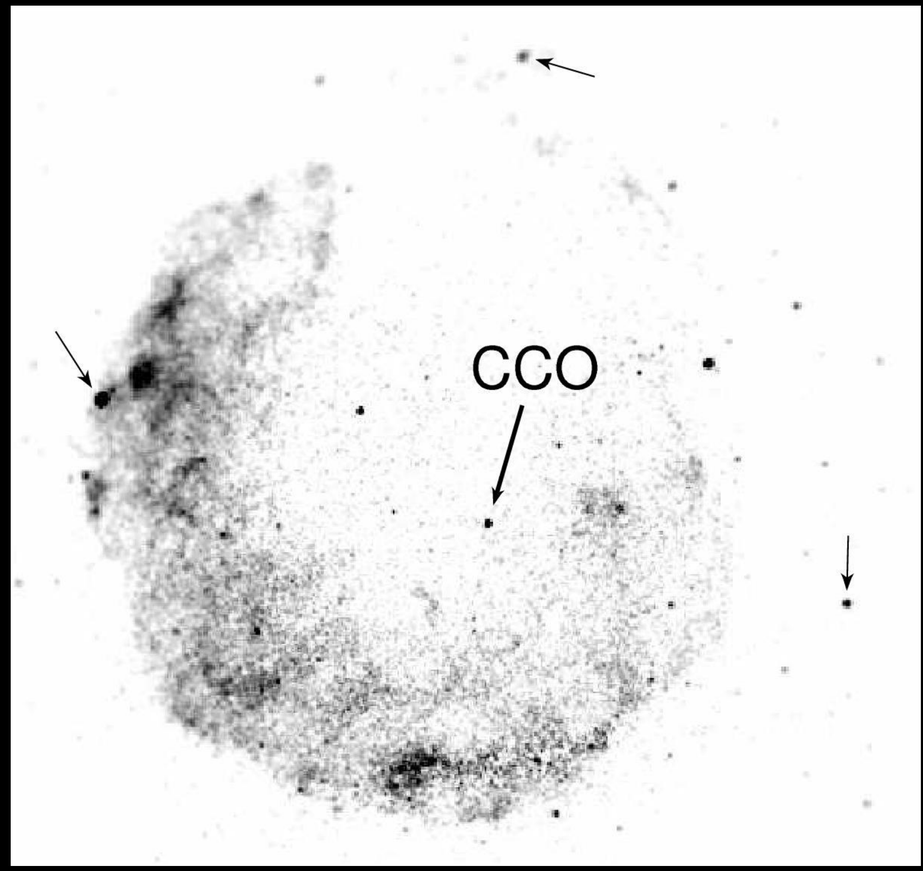

Klochkov, Suleimanov, Sasaki & Santangelo (2016)

Hidden magnetic field scenario

Strong subsurface magnetic fields buried during the SN explosion (Muslimov & Page 1995, Vigano & Pons 2012). Alternatively, small scale magnetic fields (Igoshev, Gourgouliatos & Hollerbach 2021; Gourgouliatos, Hollerbach, Igoshev 2020).

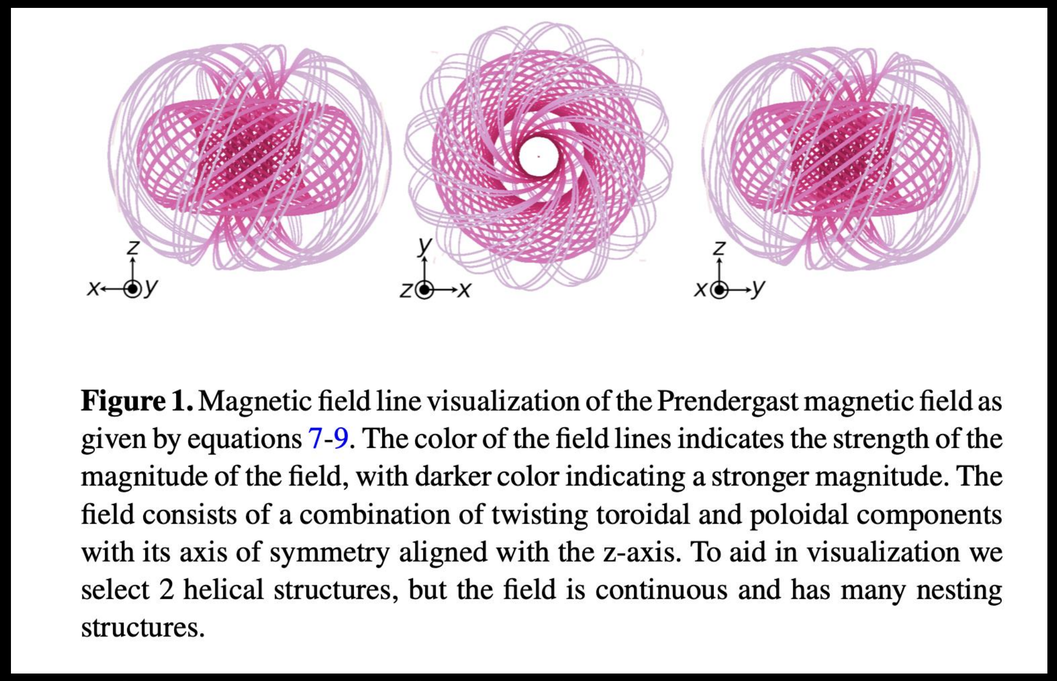

Figure 1. Magnetic field line visualization of the Prendergast magnetic field as given by equations 7-9. The color of the field lines indicates the strength of the magnitude of the field, with darker color indicating a stronger magnitude. The field consists of a combination of twisting toroidal and poloidal components with its axis of symmetry aligned with the z-axis. To aid in visualization we select 2 helical structures, but the field is continuous and has many nesting structures.

Kaufman et al. (2022) Prendergast

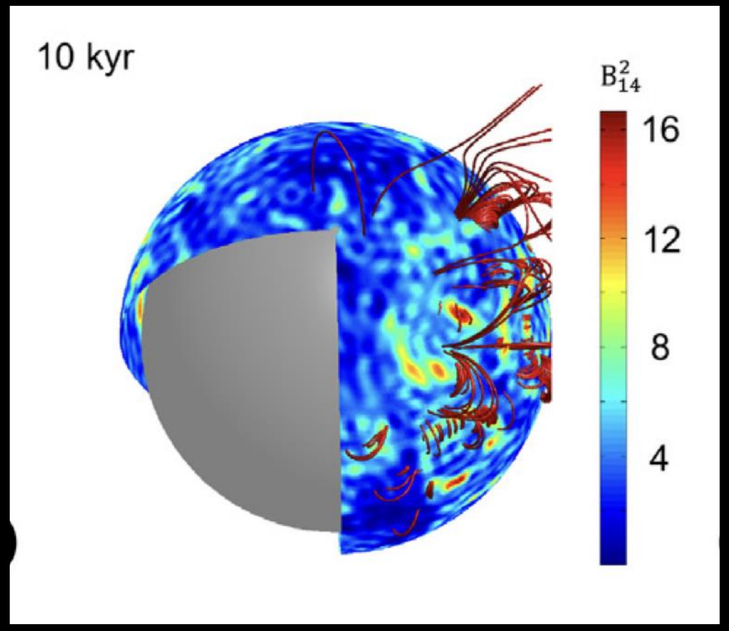

Gourgouliatos et al. (2020)

Magnetic fields of neutron stars are complex

- Magnetars probably have strong toroidal fields in the crust.
- Some low-B magnetars as well as some X-ray Dim Isolated Neutron Stars have individual arcs of strong poloidal magnetic fields.
- CCOs have hidden magnetic fields which are either buried or small scale poloidal.

Magnetic field evolution problem

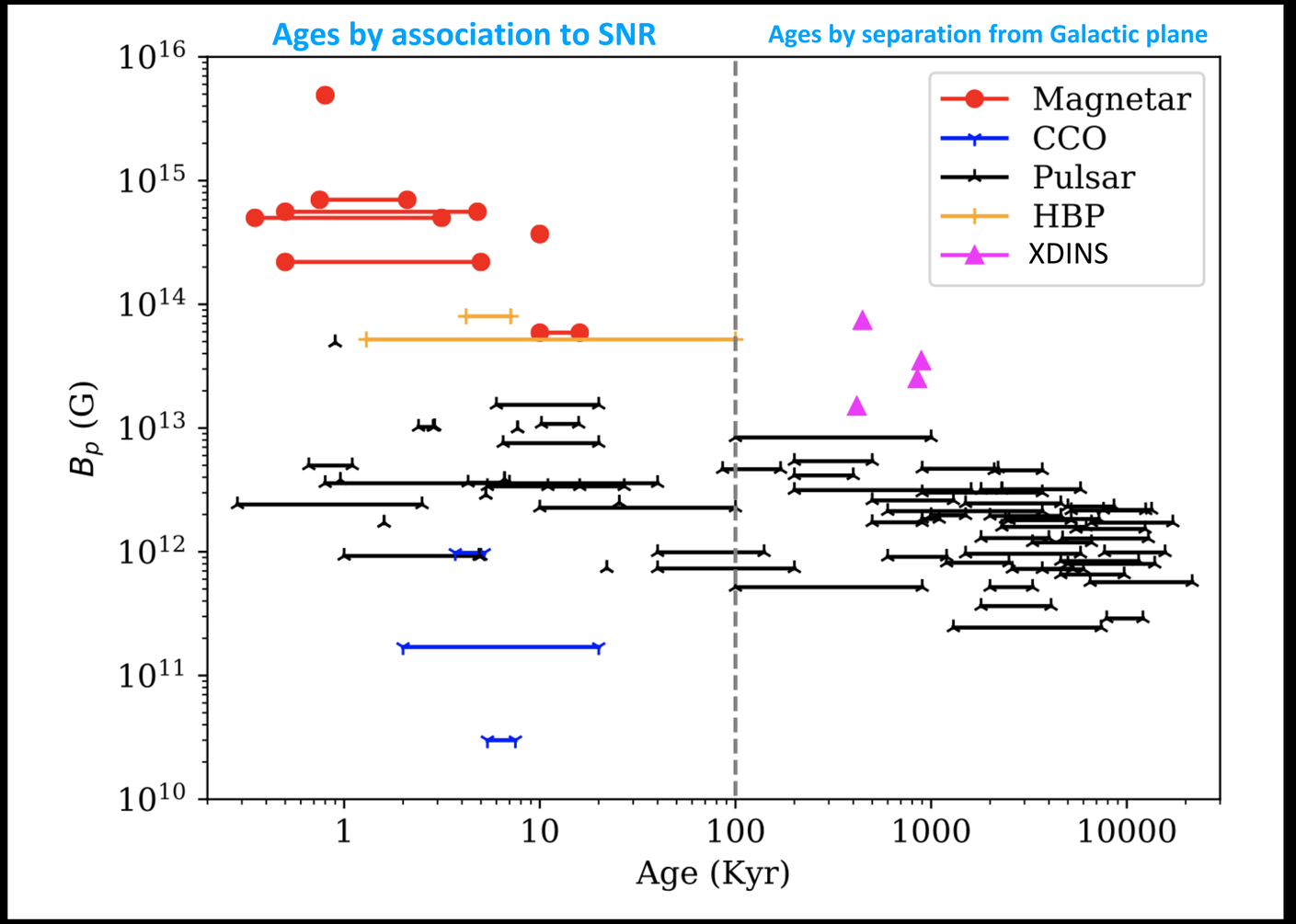

Review by Igoshev, Popov & Hollerbach (2021)

Formation of magnetic fields

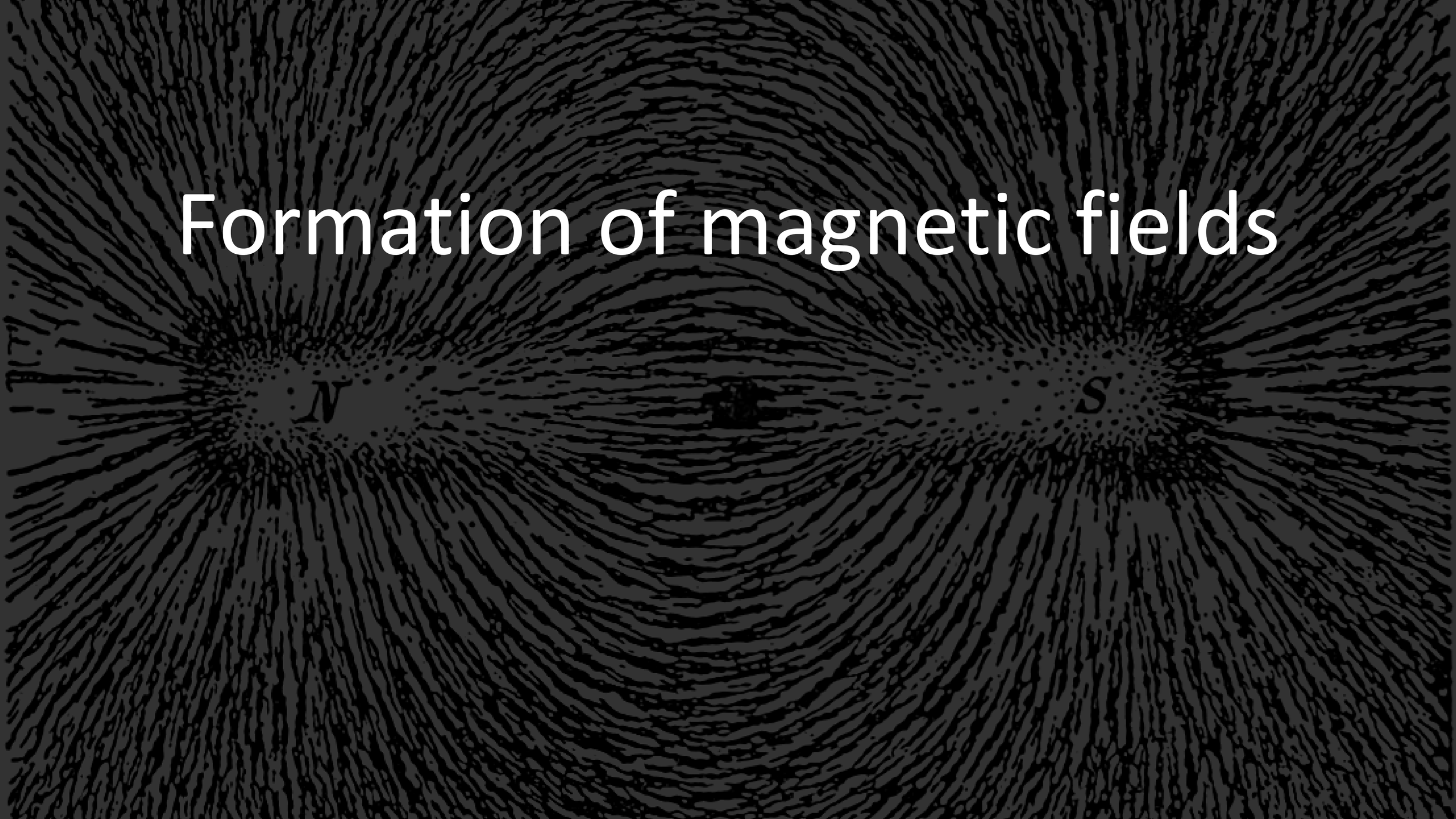

From supernova to NS

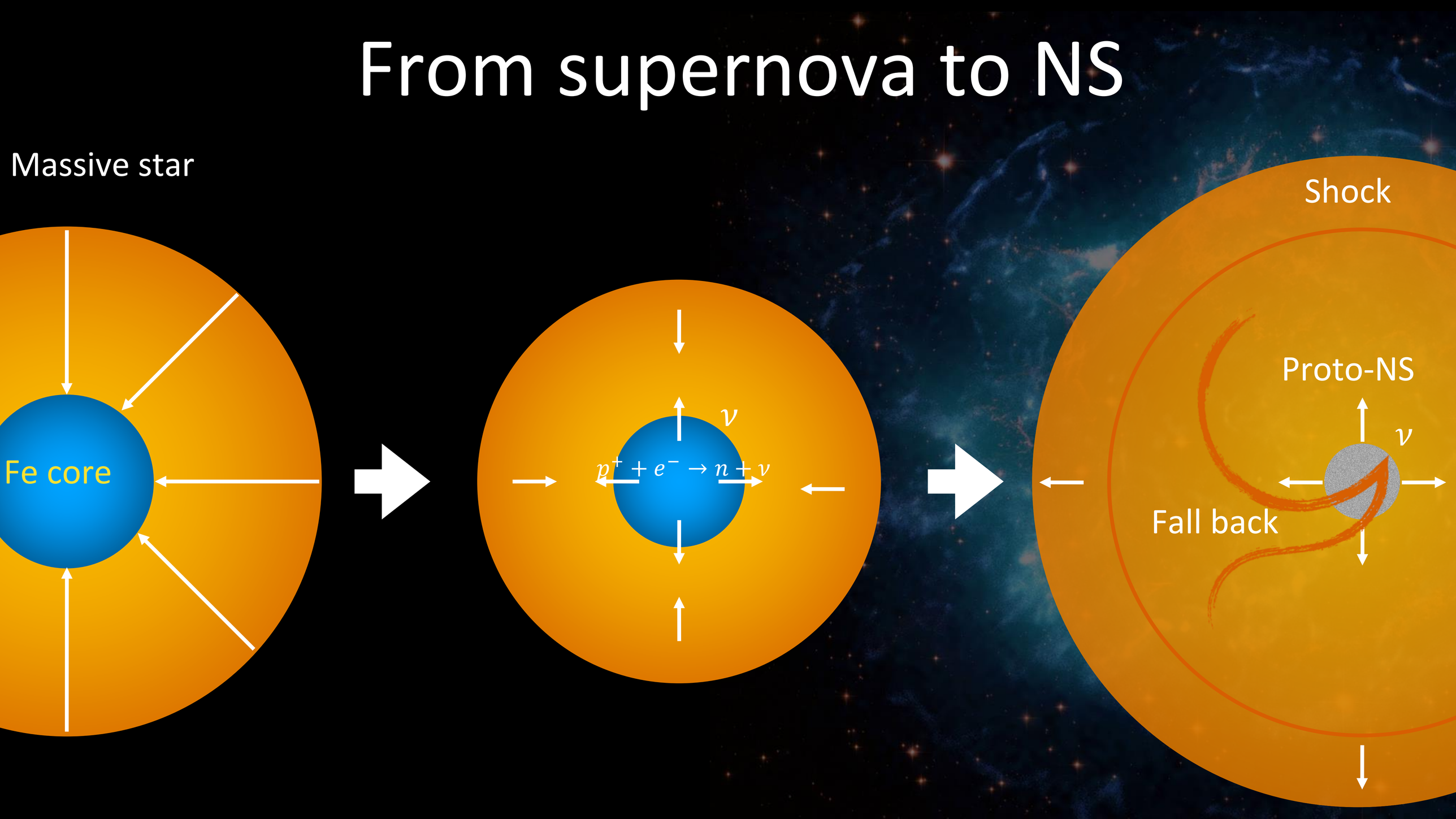

Formation of strong magnetic fields

Fossil hypothesis: magnetic field of a massive star (NS progenitors) is amplified when the magnetised core collapses.

Dynamo hypothesis: there are two regions in the proto-neutron star where convection is possible. The cooling of neutron star proceed slow enough which allows multiple dynamical overturns. (See e.g. Thompson & Murray 2001)

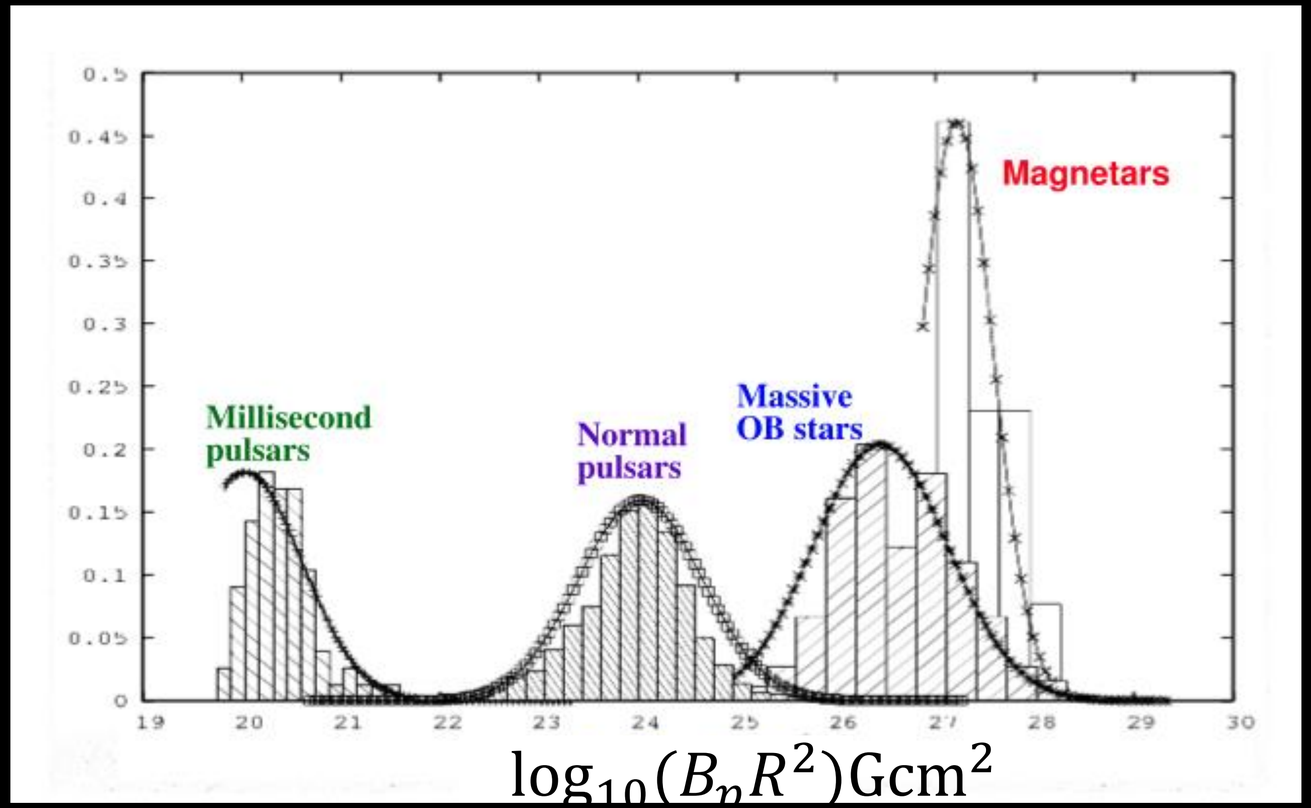

Ferrario and Wickramasinghe (2006)
Igoshev & Kholtygin (2011)
Makarenko, Igoshev & Kholtygin (2021)

Dynamo in MHD

Induction equation:

$$\frac{\partial \vec{B}}{\partial t} = \nabla \times (\vec{u} \times \vec{B}) + \eta(\nabla^2 \vec{B})$$

Some fluid velocity u which advects fields amplifying it.

Large regular velocities develop as a result of an instability:

1. Convective

2. Magneto-rotational

3. Tayler-Spruit

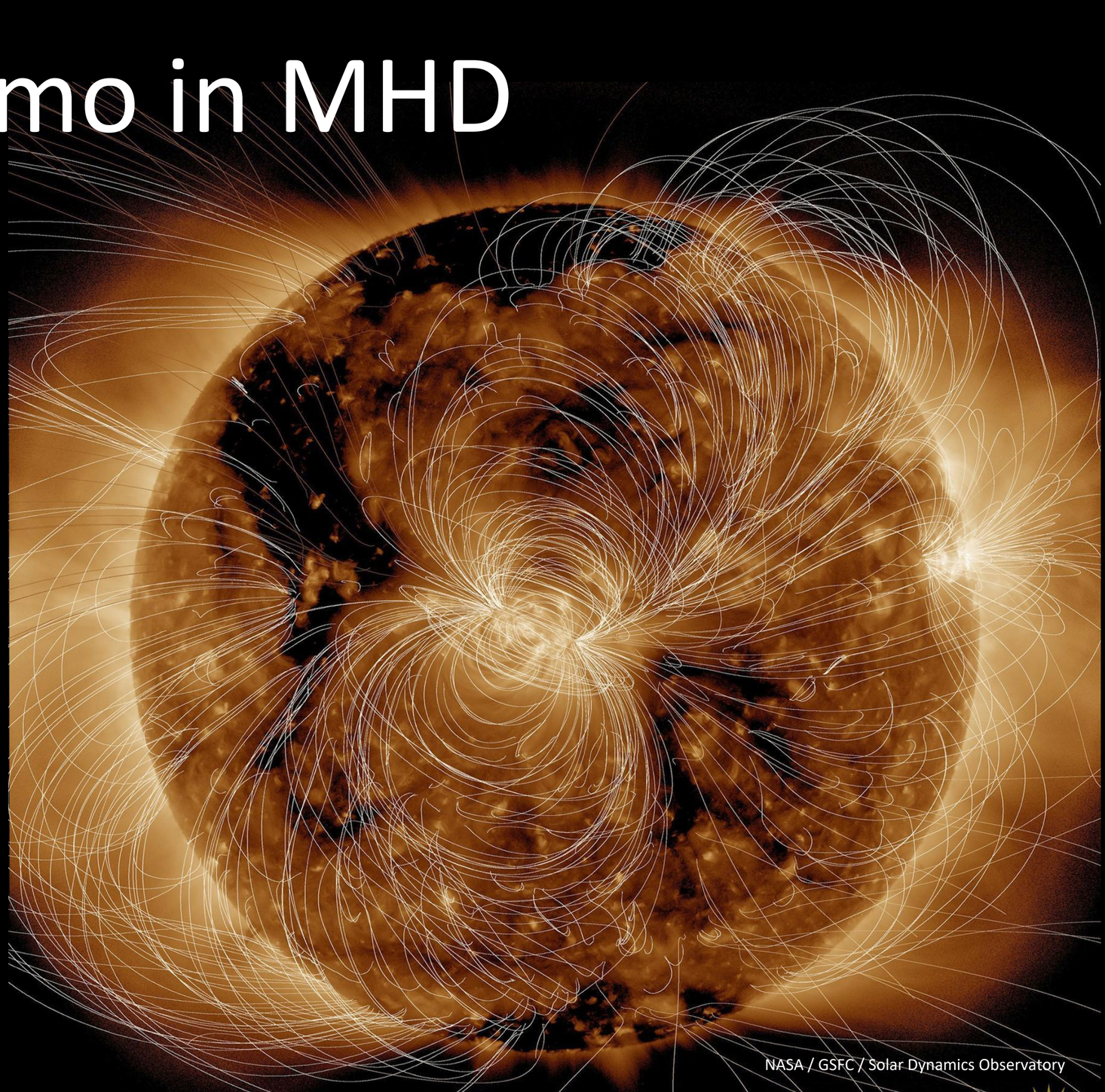

NASA / GSFC / Solar Dynamics Observatory

Proto-NS simulation: Boussinesq approximation

$$\frac{Dv}{Dt} + \frac{2}{E}\vec{e}_z \times \vec{v} = -\nabla\Pi + \frac{\mathrm{Ra}}{\mathrm{Pr}} T\vec{e}_r + \frac{1}{\mathrm{EPm}}(\nabla \times \vec{B}) \times \vec{B} + \Delta\vec{v}$$

$$\frac{\partial \vec{B}}{\partial t} = \nabla \times (\vec{v} \times \vec{B}) + \frac{1}{\mathrm{Pm}}\Delta\vec{B}$$

$$\frac{DT}{Dt} = \frac{1}{\mathrm{Pr}}\Delta T \qquad \nabla \cdot \vec{B} = 0 \qquad \nabla \cdot \vec{u} = 0$$

Convective instability

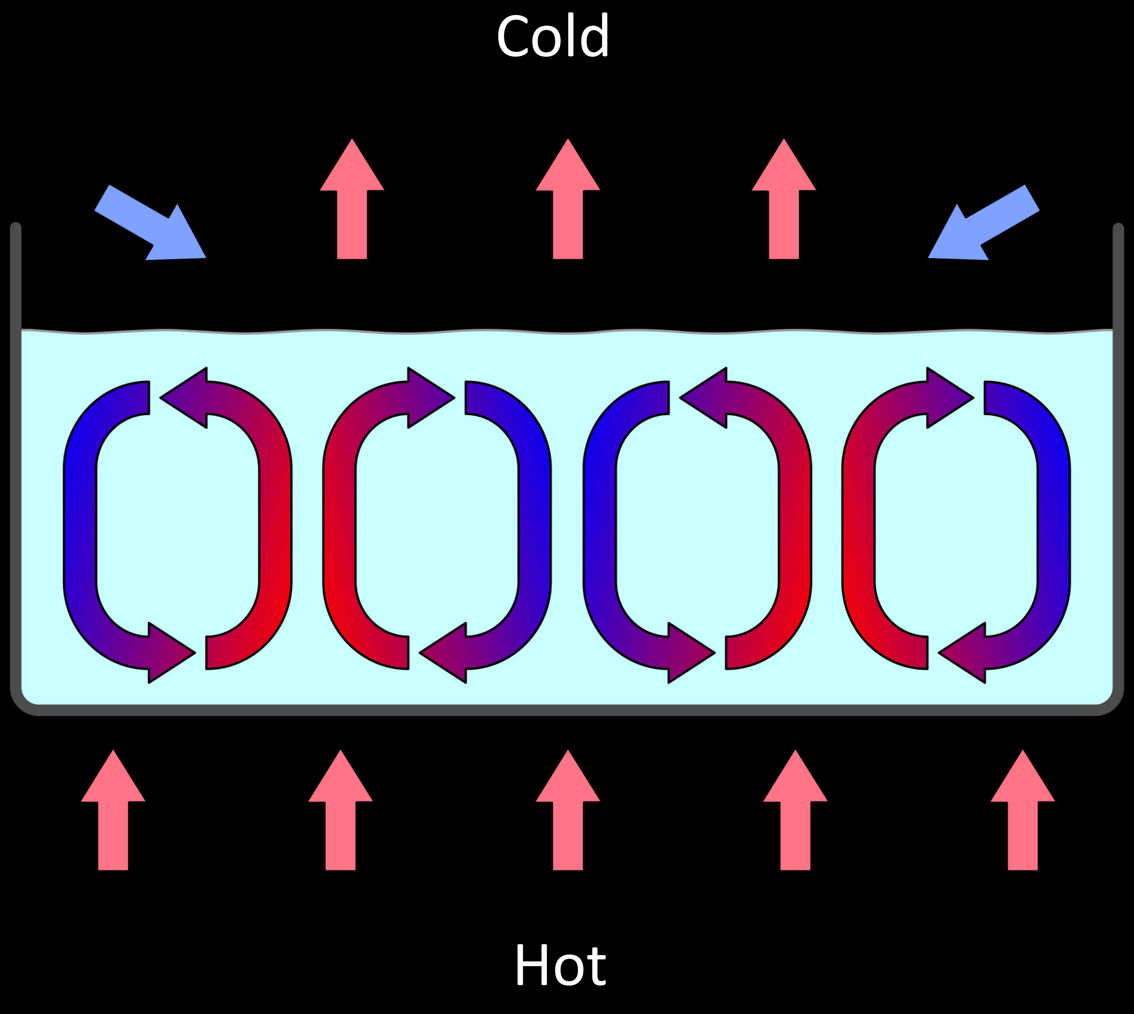

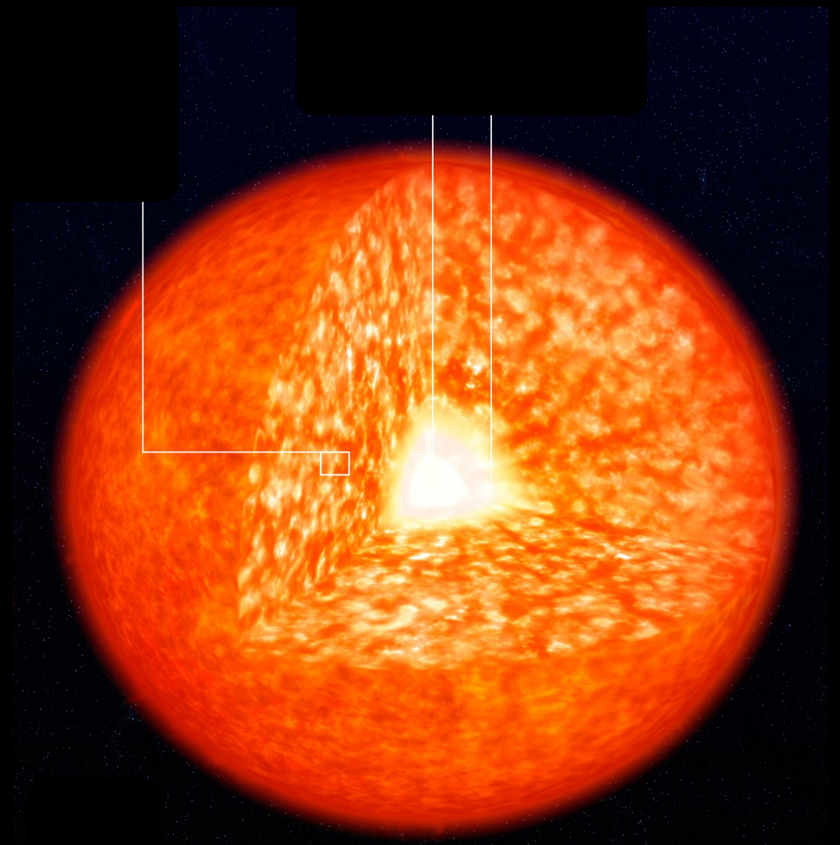

ESO

Convective instability

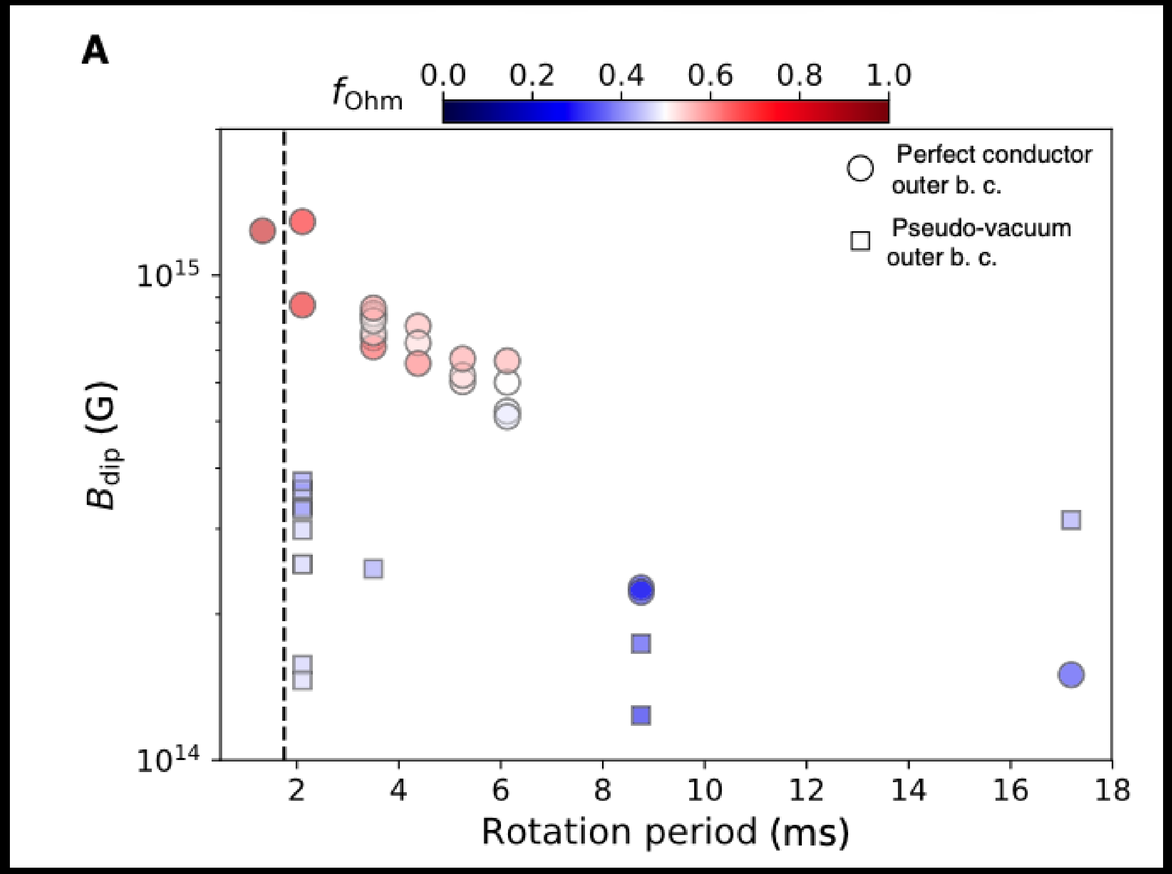

Raynaud et al. (2020)

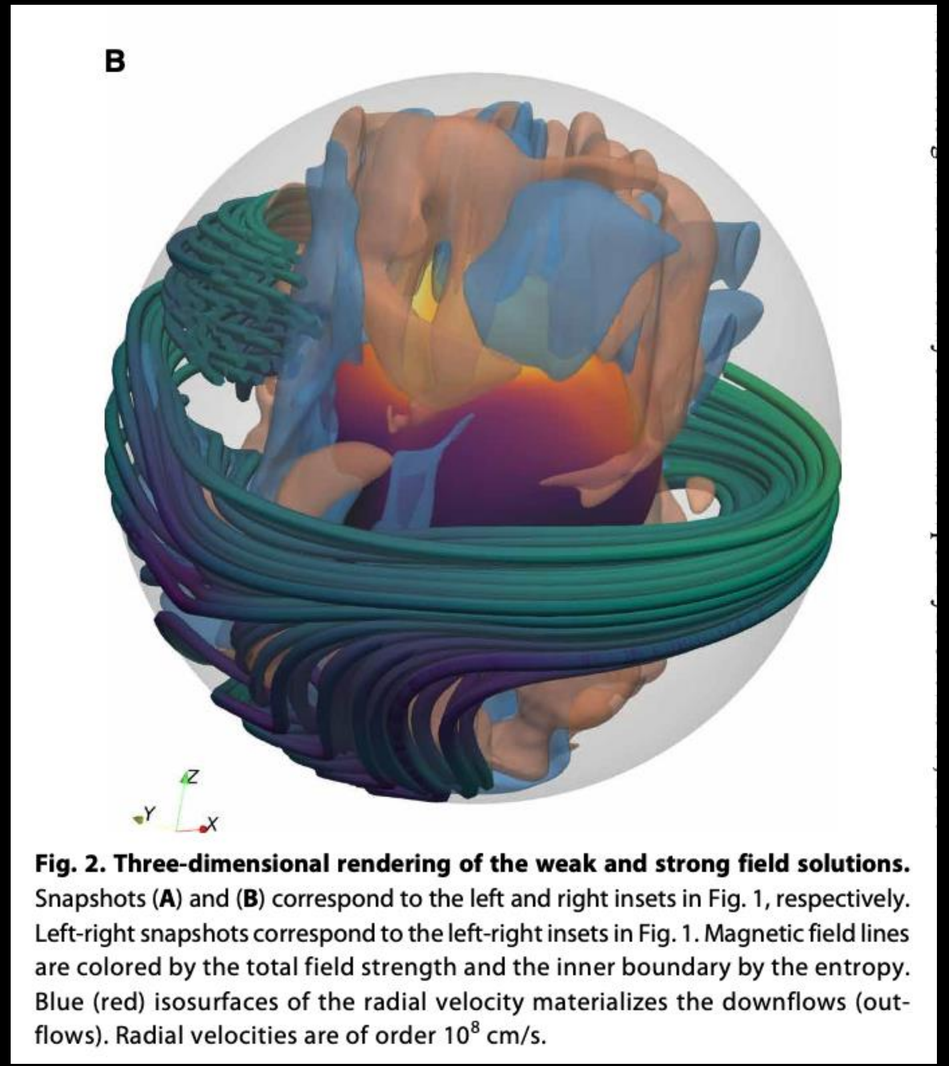

Fig. 2. Three-dimensional rendering of the weak and strong field solutions. Snapshots (**A**) and (**B**) correspond to the left and right insets in Fig. 1, respectively. Left-right snapshots correspond to the left-right insets in Fig. 1. Magnetic field lines are colored by the total field strength and the inner boundary by the entropy. Blue (red) isosurfaces of the radial velocity materializes the downflows (outflows). Radial velocities are of order 10^8 cm/s.

Magneto-rotational instability

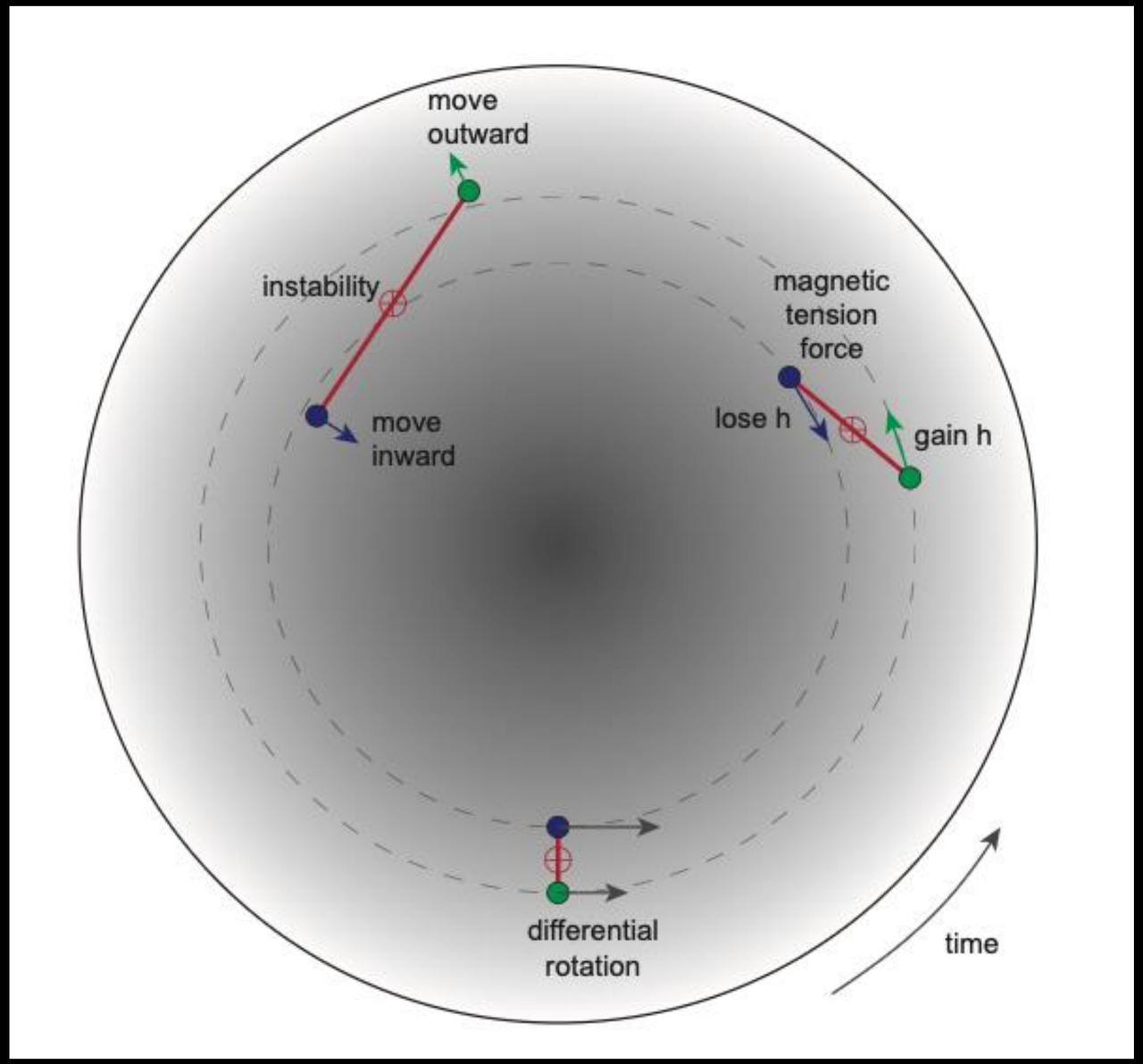

Reboul-Salze et al. (2022)

Armitage (2022). ArXiv: 2201.07262

Magneto-rotational instability

Small-scale magnetic field predominantly toroidal.

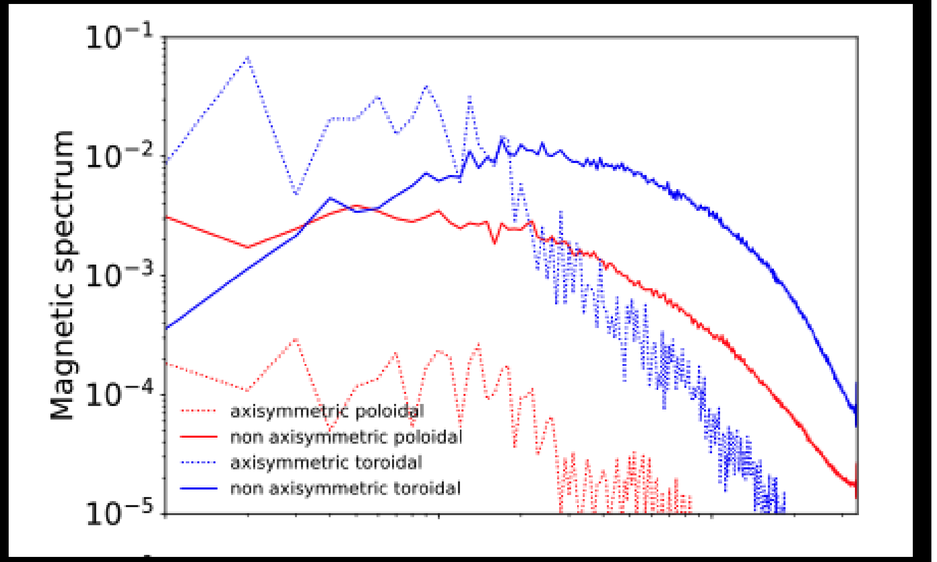

Reboul-Salze et al. (2022)

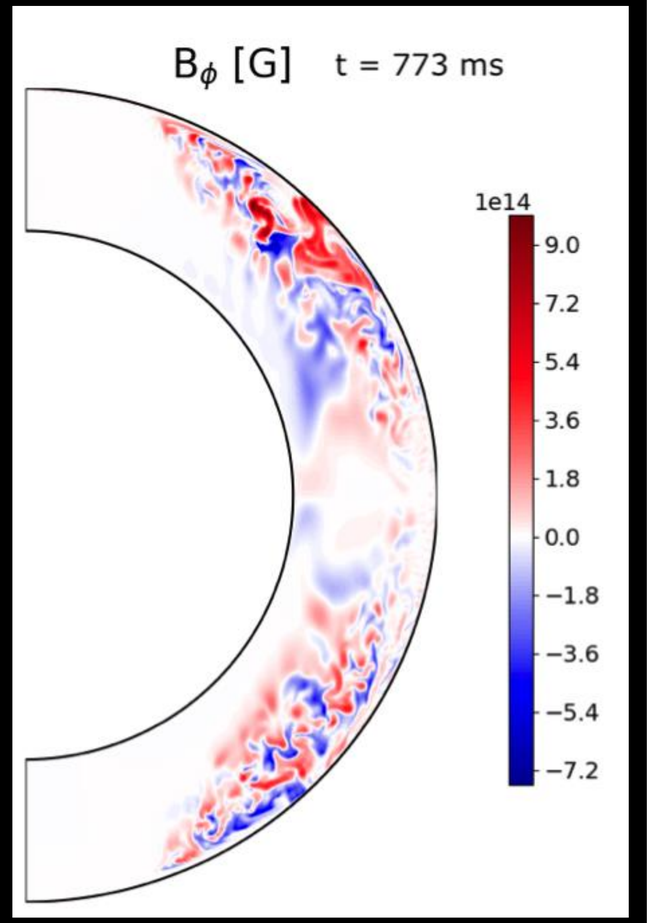

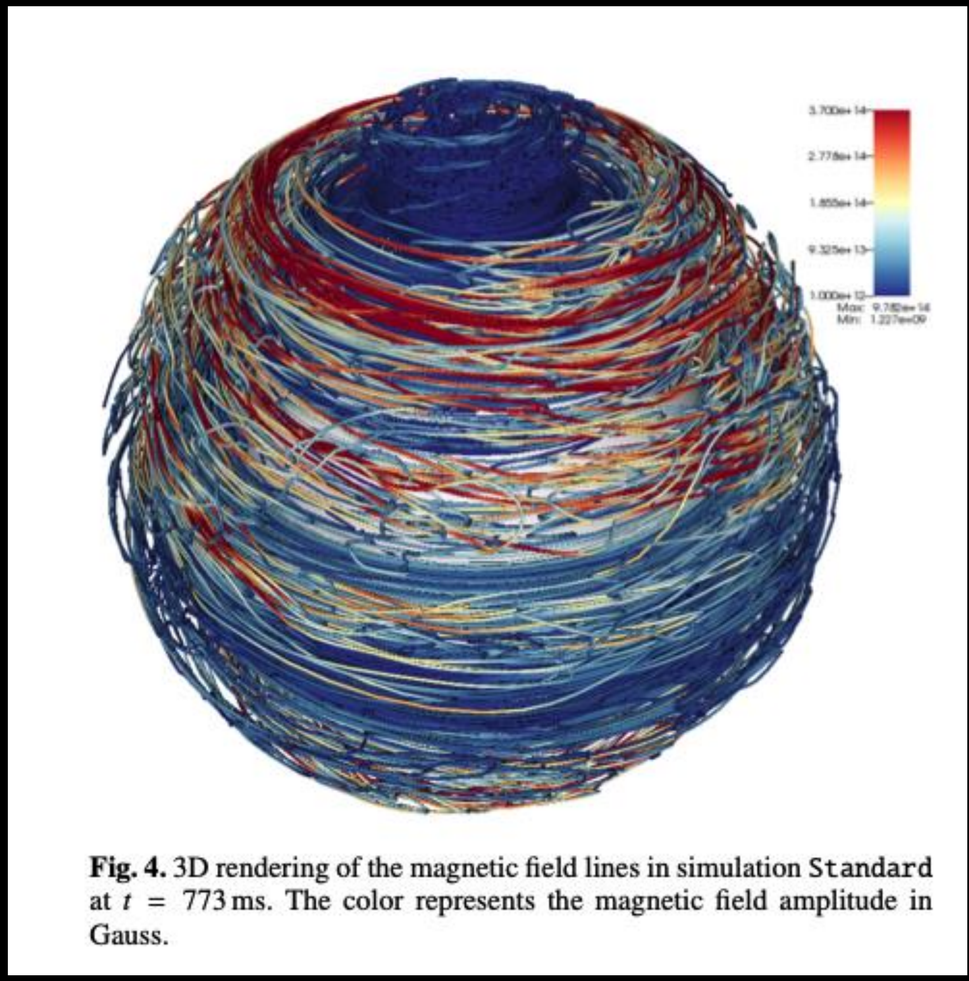

Fig. 4. 3D rendering of the magnetic field lines in simulation `Standard` at $t = 773$ ms. The color represents the magnetic field amplitude in Gauss.

Tayler-Spruit instability

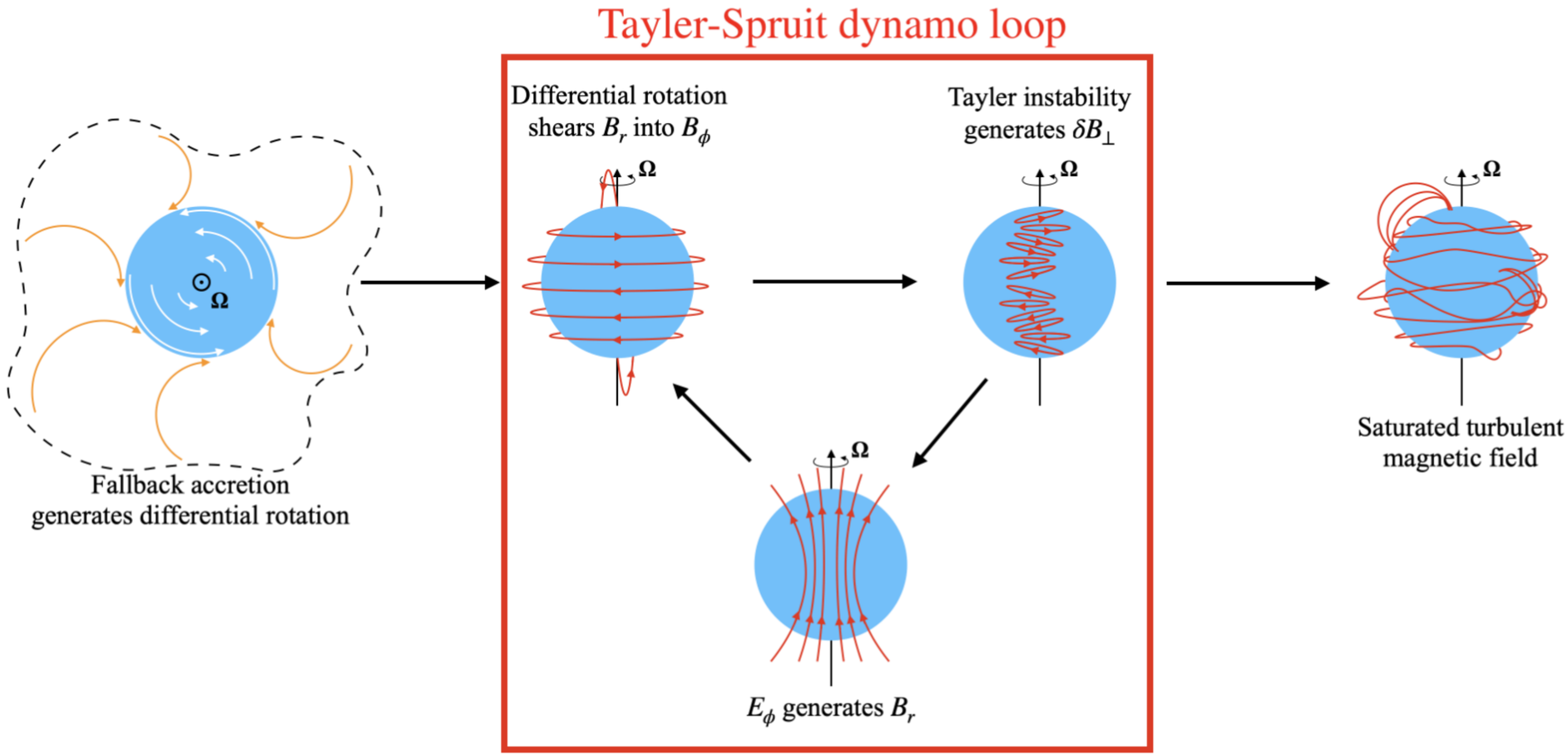

Fig. 1. Schematic representation of the different stages of our magnetar formation scenario. The dashed line encloses the region of the fallback (orange arrows). Red and white lines represent the magnetic field lines and fluid motions, respectively. $\boldsymbol{\Omega}$ and E_ϕ stand for the angular rotation frequency and the azimuthal component of the electromotive force, respectively. B_ϕ and B_r are the axisymmetric azimuthal and radial magnetic fields, and $\delta B_\perp$ is the non-axisymmetric perpendicular magnetic field.

Proto-NS simulation: Boussinesq approximation

$$\frac{Dv}{Dt} + \frac{2}{E}\vec{e}_z \times \vec{v} = -\nabla\Pi + \frac{\mathrm{Ra}}{\mathrm{Pr}} T\vec{e}_r + \frac{1}{\mathrm{EPm}}(\nabla \times \vec{B}) \times \vec{B} + \Delta\vec{v}$$

$$\frac{\partial \vec{B}}{\partial t} = \nabla \times (\vec{v} \times \vec{B}) + \frac{1}{\mathrm{Pm}}\Delta\vec{B}$$

$$\frac{DT}{Dt} = \frac{1}{\mathrm{Pr}}\Delta T \qquad \nabla \cdot \vec{B} = 0 \qquad \nabla \cdot \vec{u} = 0$$

- DNS simulation with stable stratification in Boussinesque approximation.
- Spherical Taylor-Couette configuration with positive shear
- No-slip and insulating boundary conditions.
- Ekman number $E = 10^{-5}$, magnetic Prandtl number $Pm = 1$.
- Ratio of Brunt-Väisälä frequency to the outer angular frequency $N/\Omega_0 = 0.1$
- Rossby number $Ro = 1 - \Omega_i/\Omega_o = 0.75$

Tayler-Spruit dynamo for proto-NS

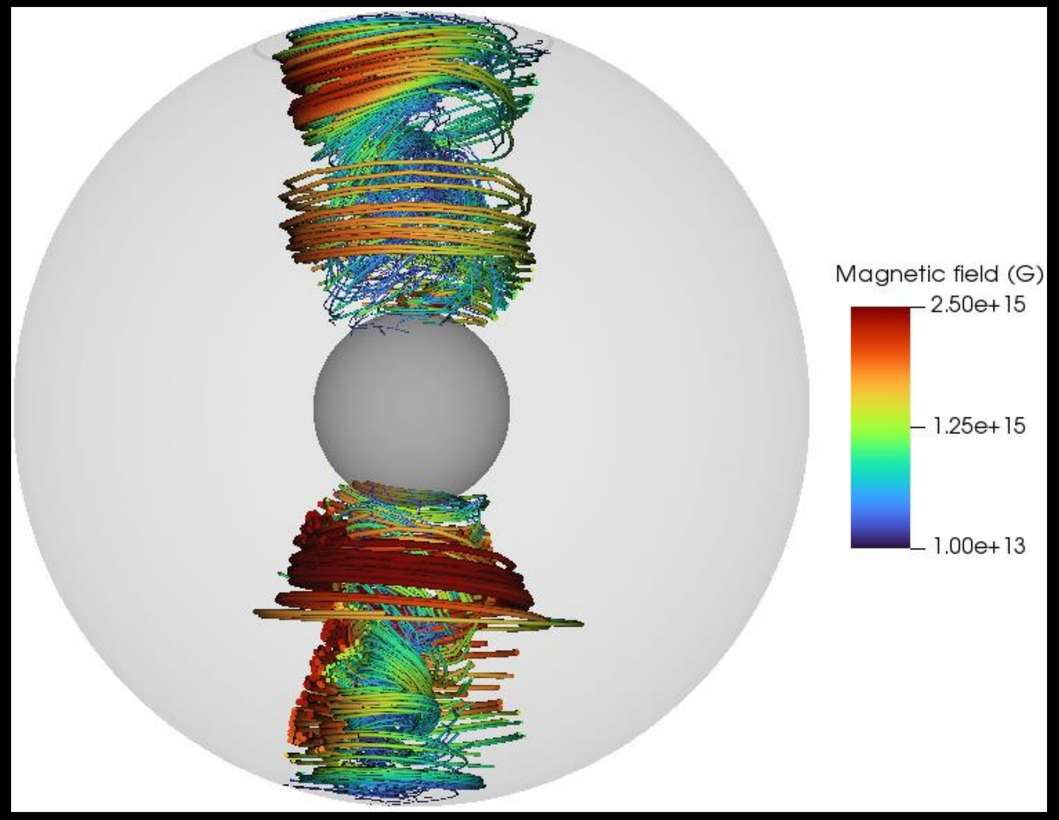

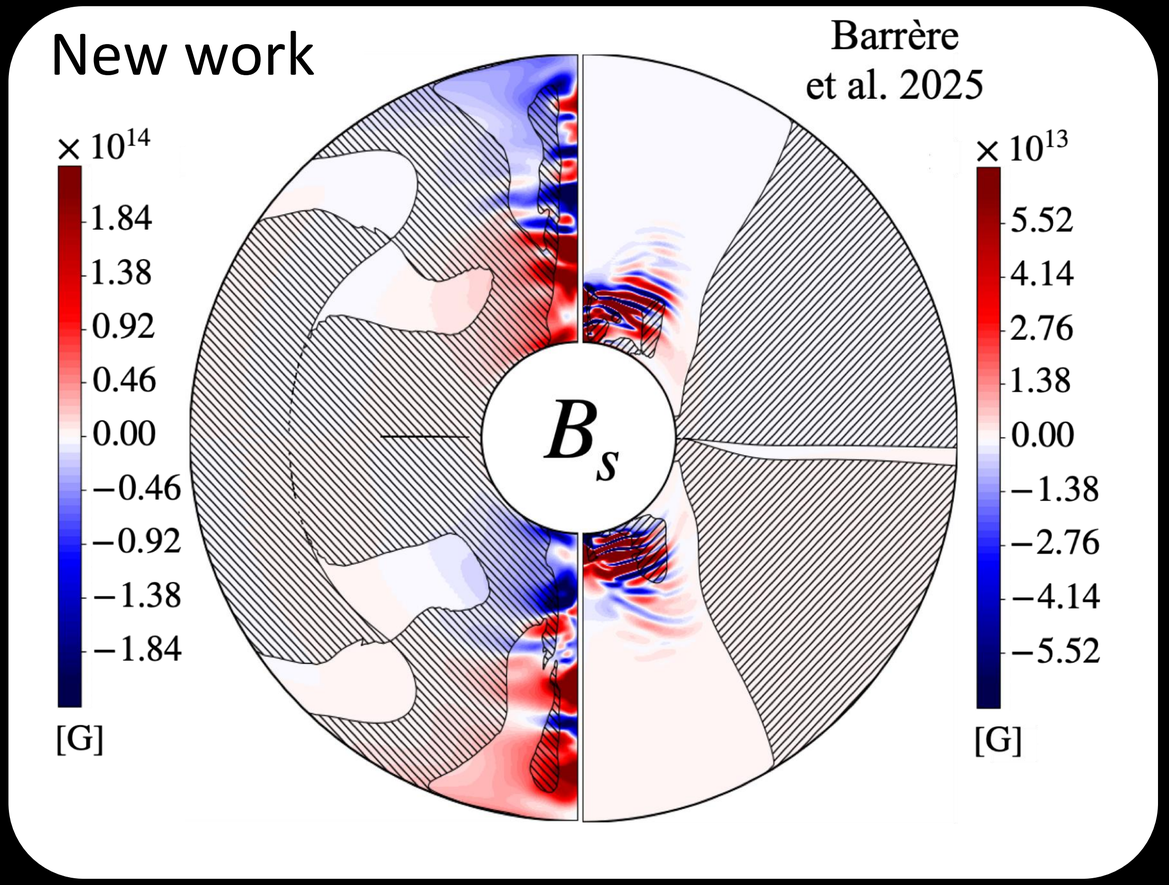

Barrère, Guiltet, Raynaud & Reboul-Salze (2023)

Barrère et al. (2025)

Proto-neutron star - exists ~30 seconds

Could have dynamo operating

Neutron star - evolves on Myr timescale

Cooling from inside via neutrino emission - no dynamo

Magnetic field evolution in neutron star crust

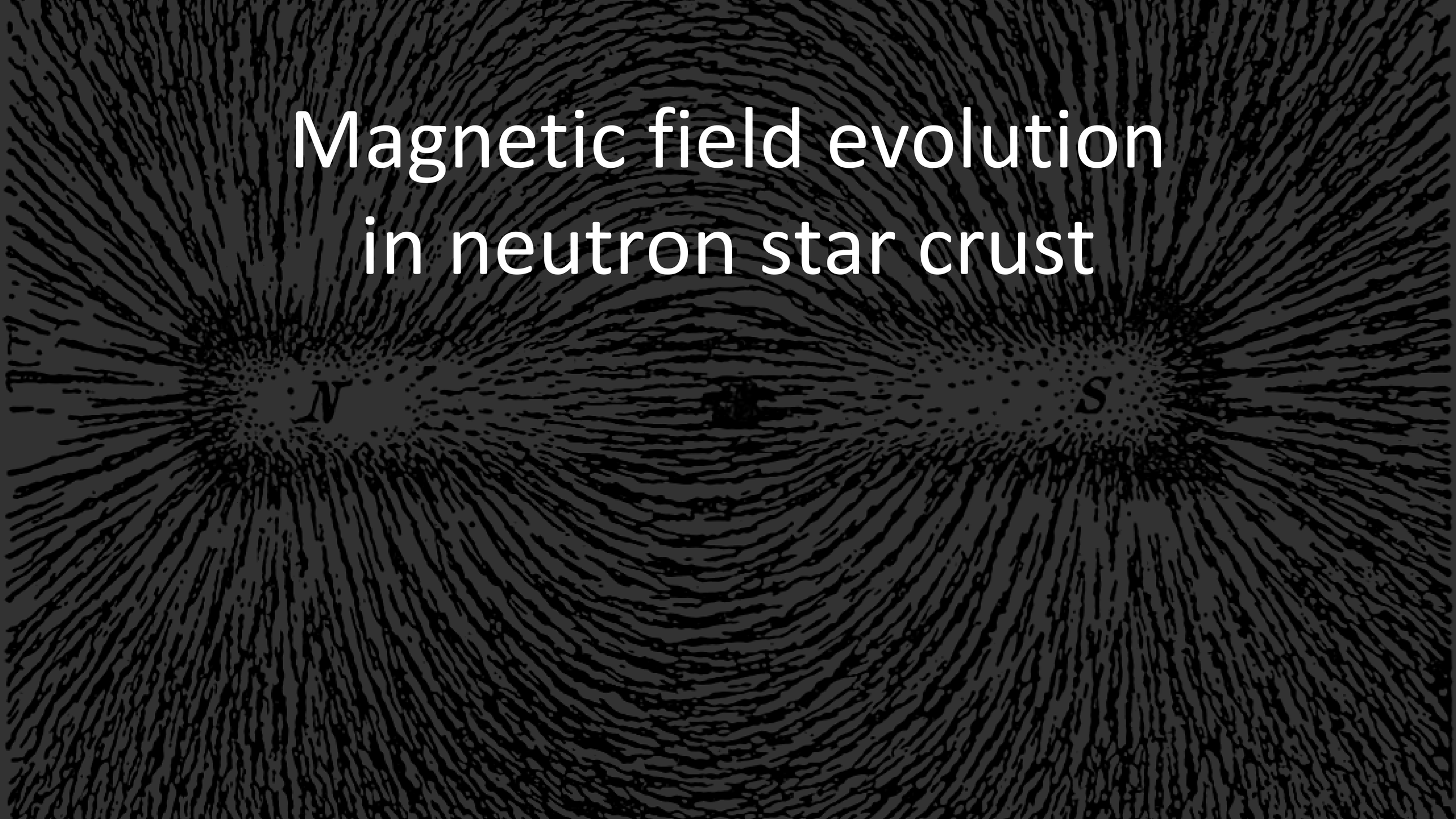

Magneto-thermal evolution of neutron stars

PARODY code

- We use the modified PARODY code to solve two equations simultaneously using the spectral decomposition for angular variables and finite difference scheme for radial direction.
- The equations are solved in a spherical shell which represents the neutron star crust. The shell extends for approximately 1 km in depth.

$$\frac{\partial \vec{B}}{\partial t} = Se\,\nabla\left(\frac{1}{\mu}\right) \times \nabla T^2 + Ha\nabla \times \left[\frac{1}{\mu^3}\vec{B} \times (\nabla \times \vec{B})\right] - \nabla \times \left[\frac{1}{\mu^2}\nabla \times \vec{B}\right]$$

Magnetic induction

$$\frac{1}{Ro}\frac{C_v}{T}\frac{\partial T^2}{\partial t} = \nabla \cdot (\mu^2 \hat{\chi} \cdot \nabla T^2) + \frac{Pe}{Se}\frac{|\nabla \times \vec{B}|^2}{\mu^2} + Pe\mu(\nabla \times B) \cdot \nabla\left(\frac{T^2}{\mu^2}\right)$$

Thermal diffusion

De Grandis et al. (2020)

Igoshev et al. (2021), Nature Astronomy

Igoshev et al. (2021), ApJ

Magneto-thermal evolution of neutron stars

PARODY code

- We use the modified PARODY code to solve two equations simultaneously using the spectral decomposition for angular variables and finite difference scheme for radial direction.
- The equations are solved in a spherical shell which represents the neutron star crust. The shell extends for approximately 1 km in depth.

$$\frac{\partial \vec{B}}{\partial t} = \underbrace{Se\,\nabla\left(\frac{1}{\mu}\right)\times\nabla T^2}_{\text{Biermann battery}} + \underbrace{Ha\nabla\times\left[\frac{1}{\mu^3}\vec{B}\times(\nabla\times\vec{B})\right]}_{\text{Hall term}} \underbrace{-\nabla\times\left[\frac{1}{\mu^2}\nabla\times\vec{B}\right]}_{\text{Ohmic term}}$$

Magnetic induction

$$\frac{1}{Ro}\frac{C_v}{T}\frac{\partial T^2}{\partial t} = \underbrace{\nabla\cdot(\mu^2\hat{\chi}\cdot\nabla T^2)}_{\text{Thermal diffusion}} + \frac{Pe}{Se}\frac{|\nabla\times\vec{B}|^2}{\mu^2} + Pe\mu(\nabla\times B)\cdot\nabla\left(\frac{T^2}{\mu^2}\right)$$

Thermal diffusion

Initial and boundary condition

- Upper boundary condition:
  - $\nabla \times B = 0$ Force-free
  - $\frac{\pi^2 k_B^2}{6e^2} \vec{r} \cdot \hat{\chi} \cdot \nabla T_b^2 = \sigma_B T_s^4$ where $\left(\frac{T_s}{10^6}\right)^2 = \left(\frac{T_b}{10^8}\right)$
    Blackbody emission from the atmosphere
- Lower boundary condition
  - $B_r = 0$ the Meissner condition
  - $\frac{\partial T}{\partial t} = 0$ no cooling

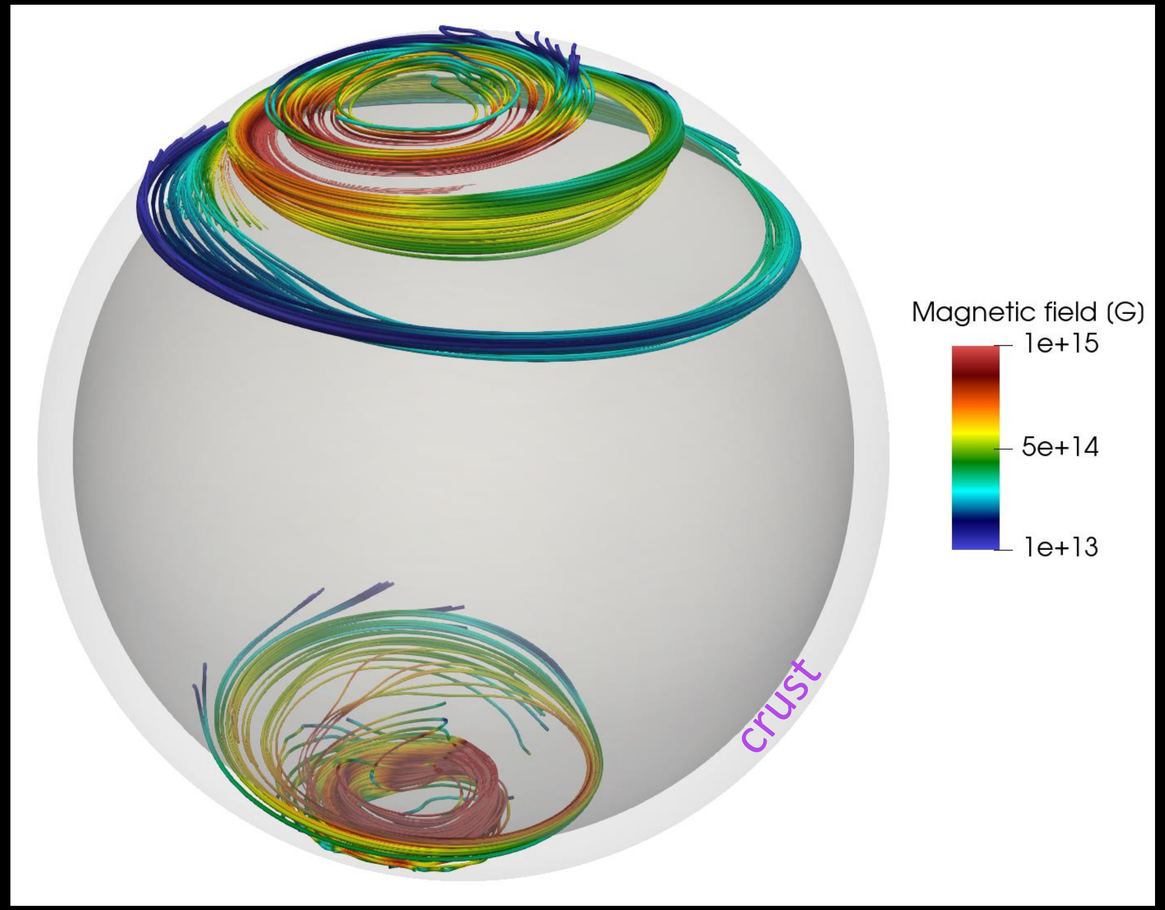

External magnetic field

Age 200 kyr

- Magnetic field structure is dominated by small scale fields. A system of magnetic arcs is formed.
- Magnetic field strength at the footpoints of individual arcs reaches 10^{14} G, the dipolar field stays low $\approx 10^{12}$ G.
- Hot regions are large and have insufficient temperature to be detected as quiescent emission.
- Surface can be heated by magnetospheric currents $\vec{J} = \vec{\nabla} \times \vec{B}$, force-free condition $\vec{\nabla} \times \vec{B} = \mu \vec{B}$ which means $J_r \propto B_r$ Regions with the strongest radial magnetic field can be heated by magnetospheric currents. Detailed future modelling is necessary.

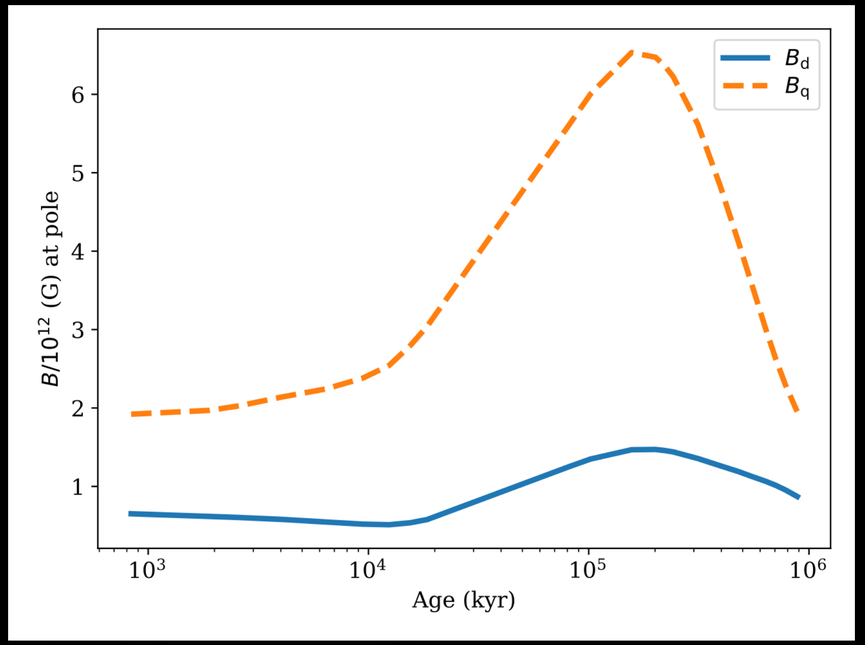

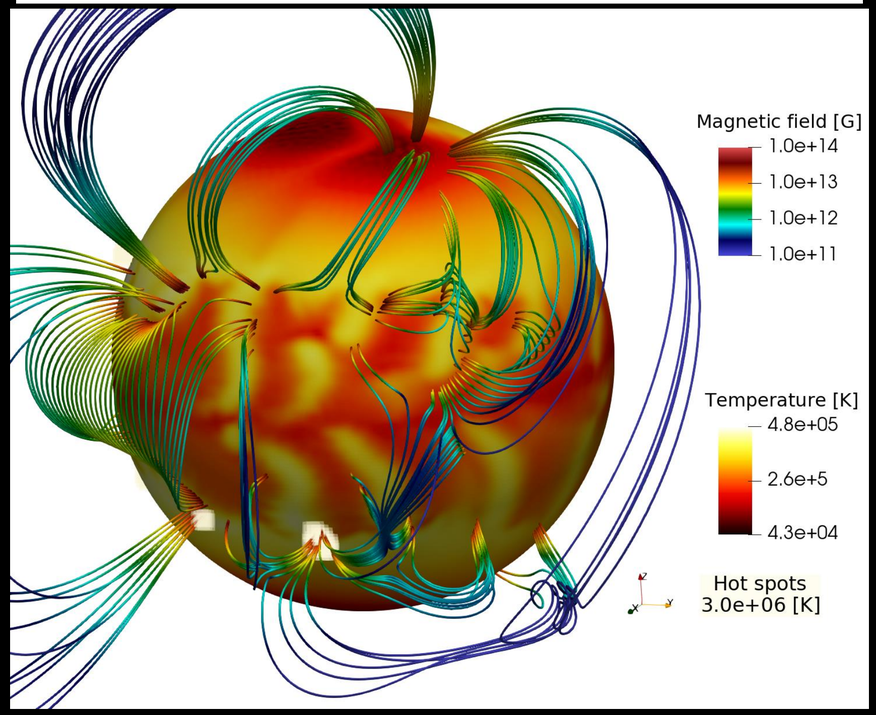

Is it a magnetar?

Crust yielding criterion

- Crust will fail near the original magnetic pole and can trigger outbursts similar to magnetar outburst with energies up to 2×10^{39} erg.

Lander & Gourgouliatos (2019) model

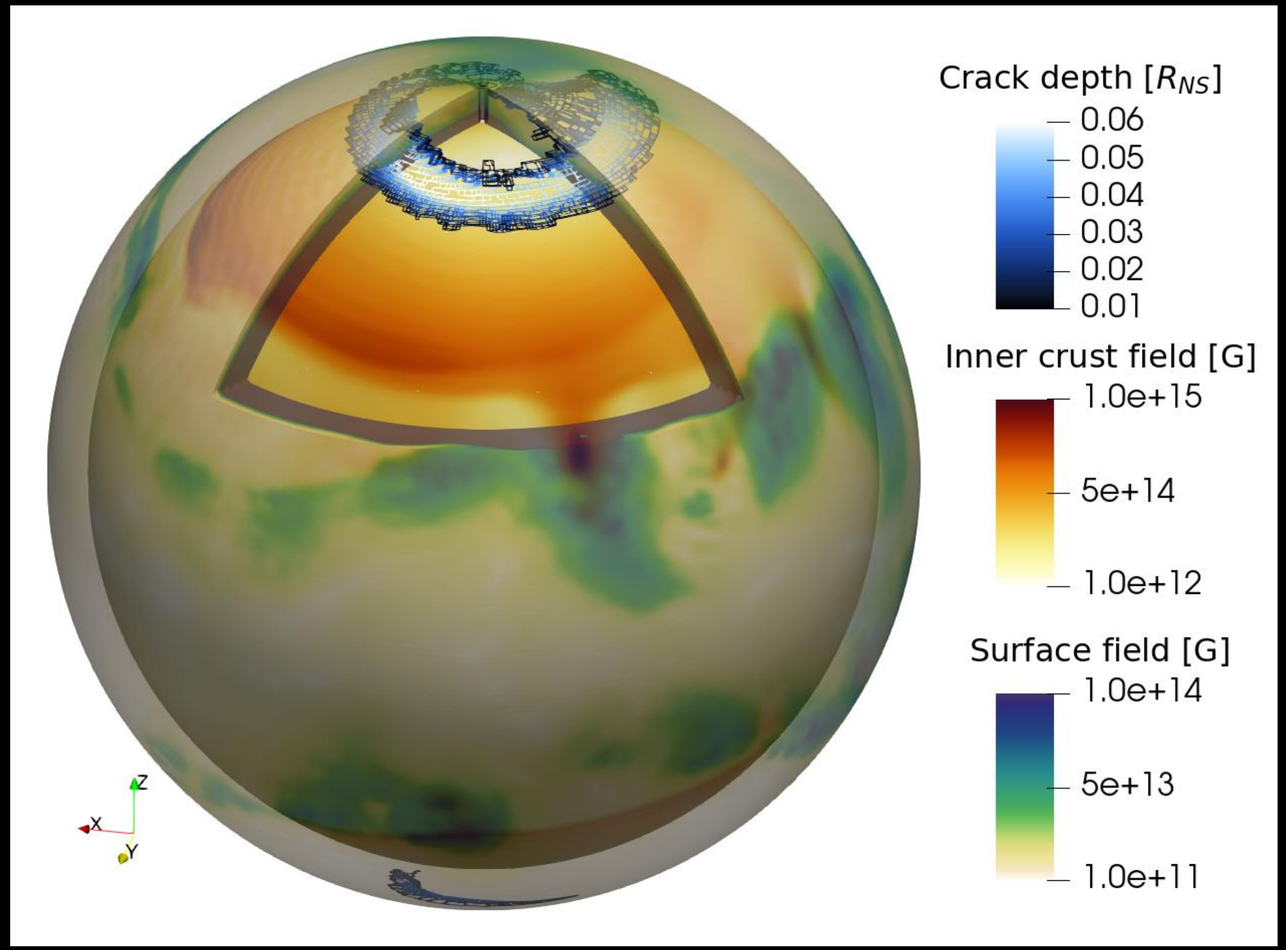

Spin period

Fallback disk

- Long periods > 1sec cannot be reached using the dipolar braking.
- Tayler-Spruit dynamo requires significant fallback accretion to operate.
- If fallback continues, it will decelerate neutron star in the propeller regime. The neutron star reaches spin periods ~ 10 sec by 200 kyr.
- Simulations based on Gompertz et al. (2014) and Ronchi, Rea, Graber et al. (2022) but with $\dot{M}_0 = 6.5 \times 10^{29}$ g/s based on TS dynamo simulations.

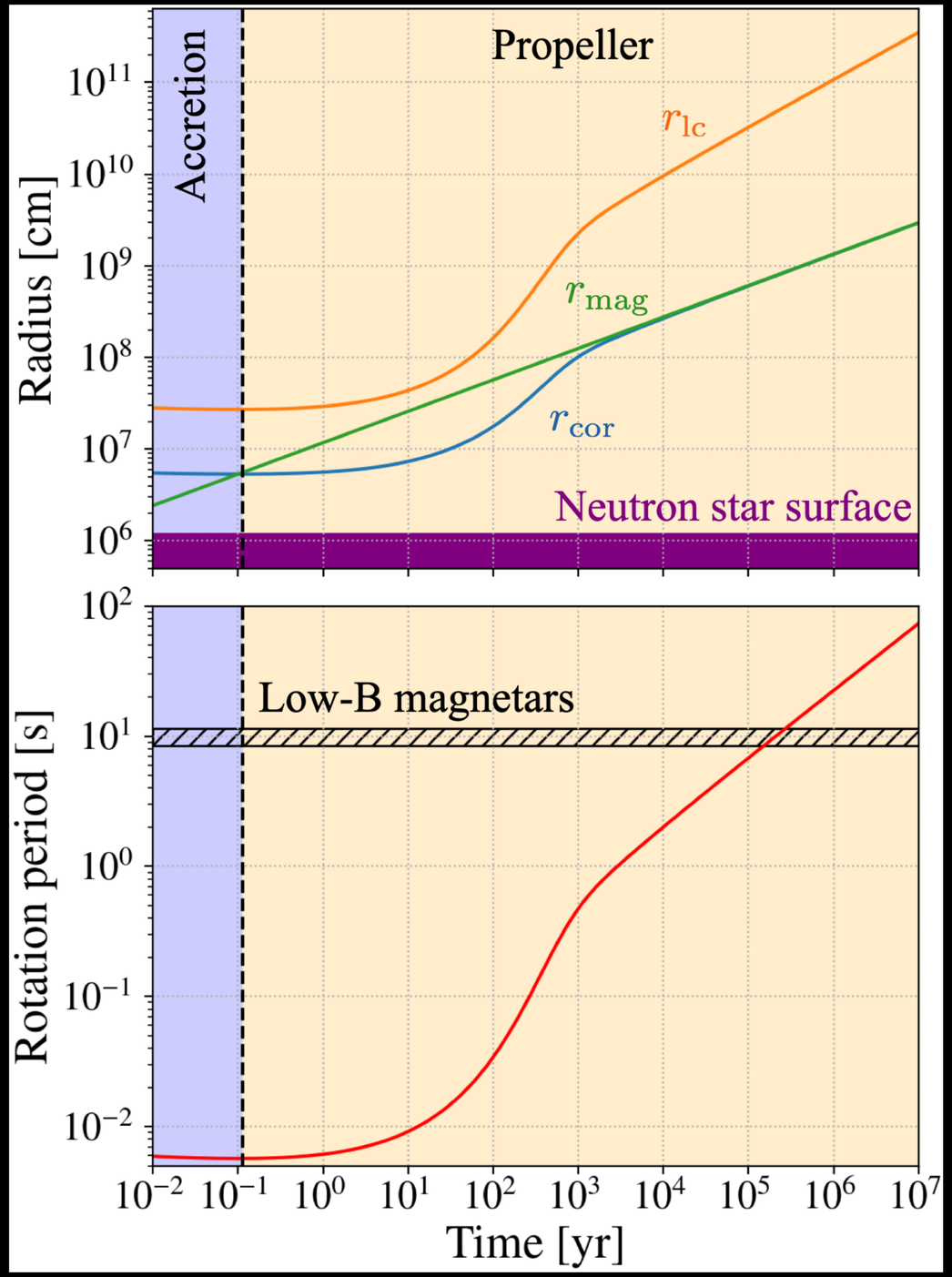

Spin period

Fallback disk

- The period derivative depends on the state of the fallback disk. If the fallback disk is partially (completely) depleted, the period derivative is closer to magnetospheric spin-down.

- At older ages these objects could turn into long-period pulsars.

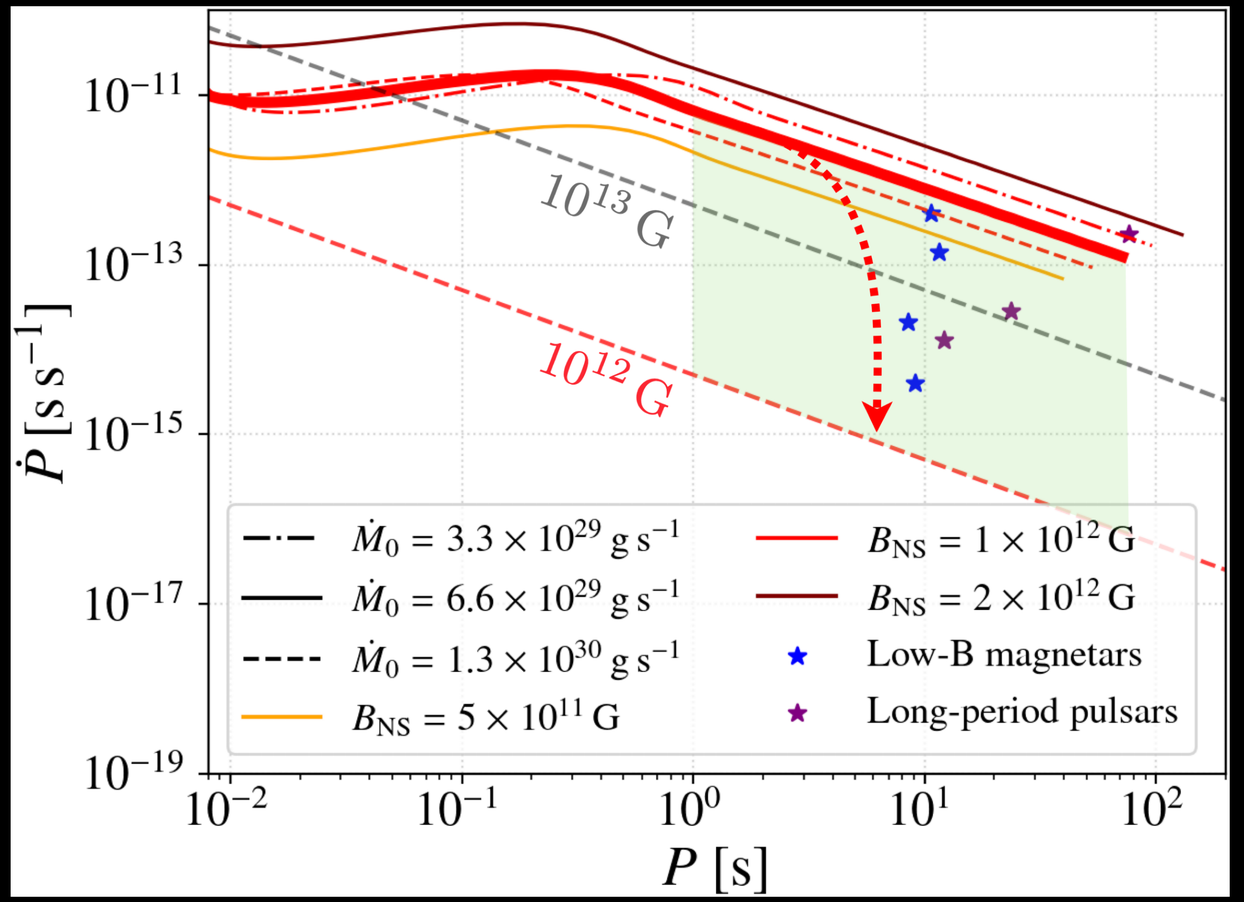

New volumetric forcing

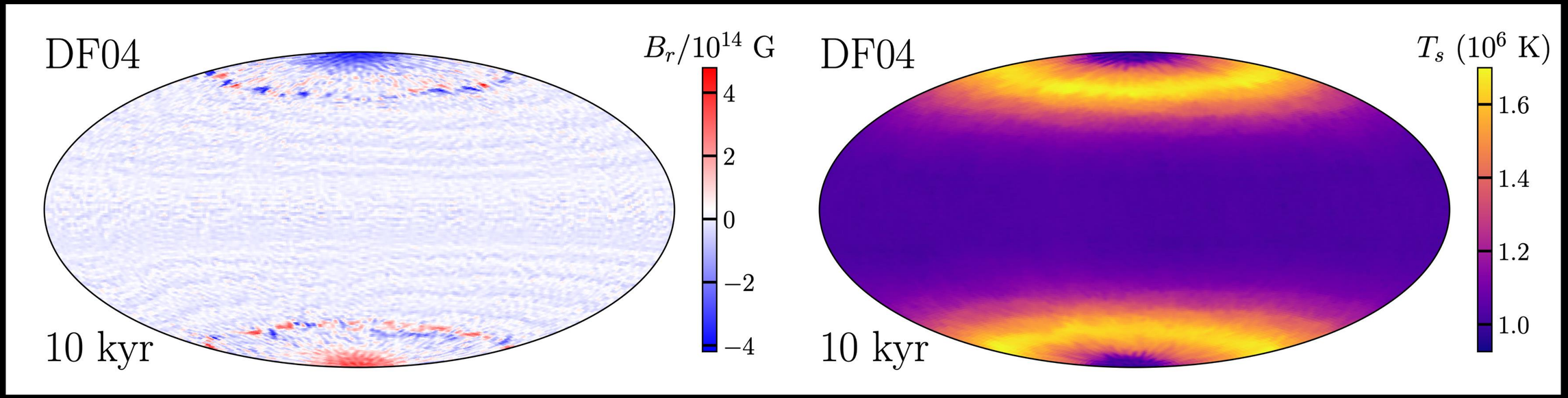

MRI dynamo

- Dehman et al. (2023) found no growth of dipolar magnetic field, however X-ray luminosities are enhanced and could explain CCOs.

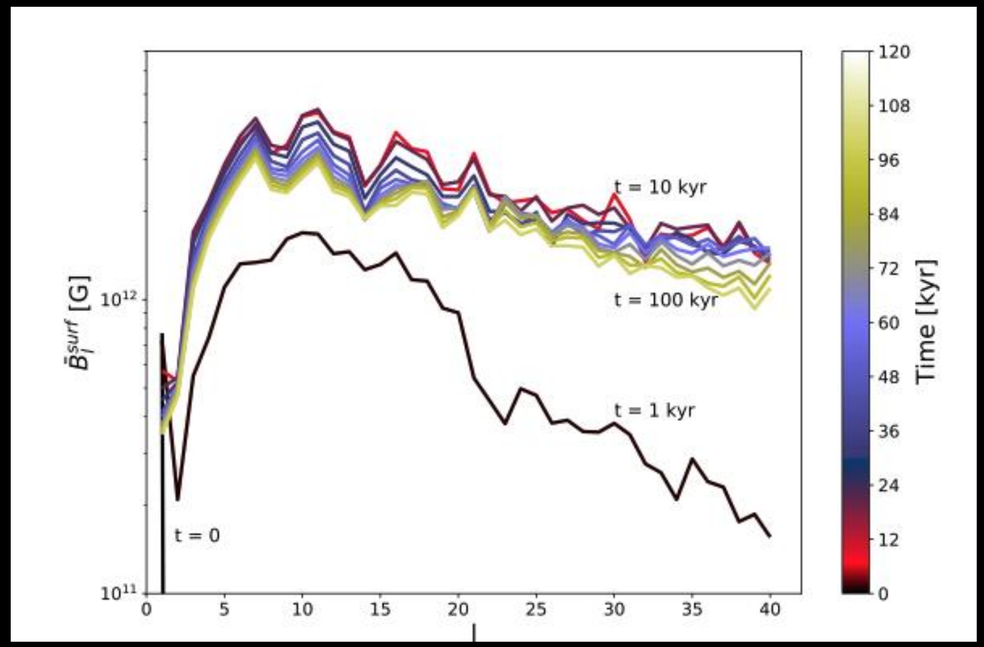

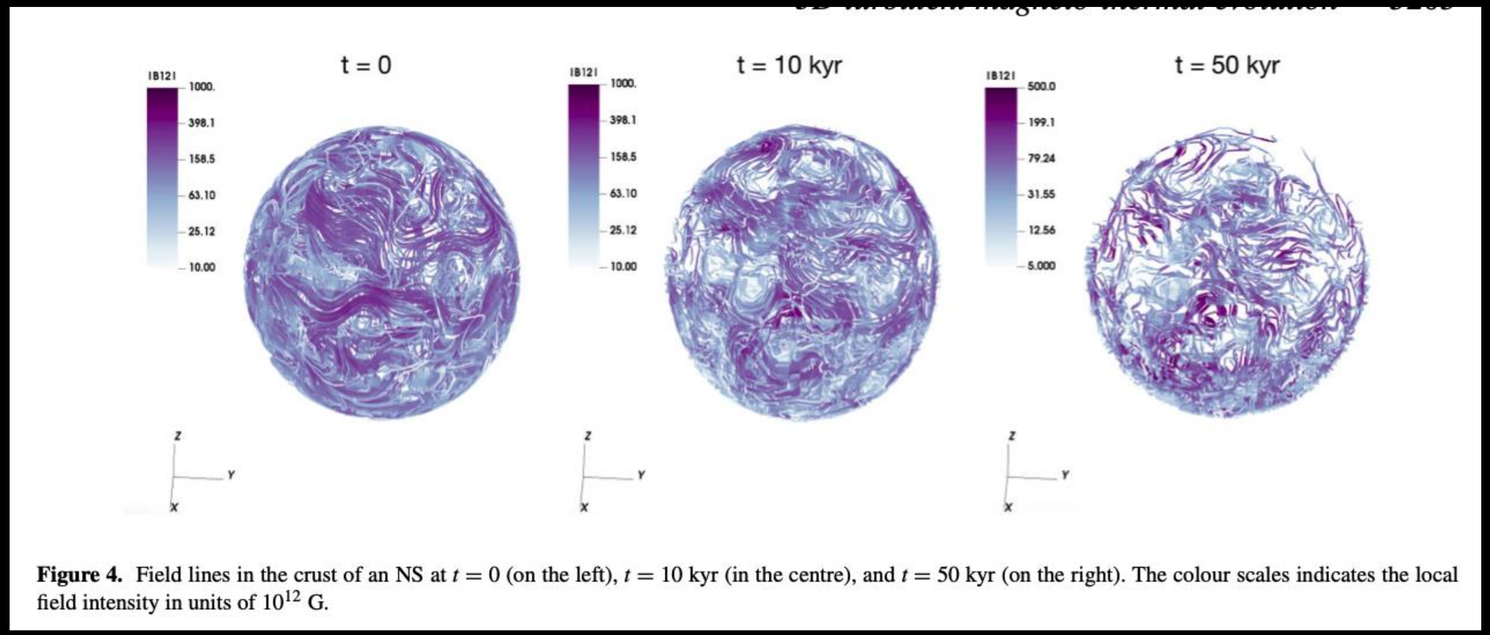

Figure 4. Field lines in the crust of an NS at $t = 0$ (on the left), $t = 10$ kyr (in the centre), and $t = 50$ kyr (on the right). The colour scales indicates the local field intensity in units of 10^{12} G.

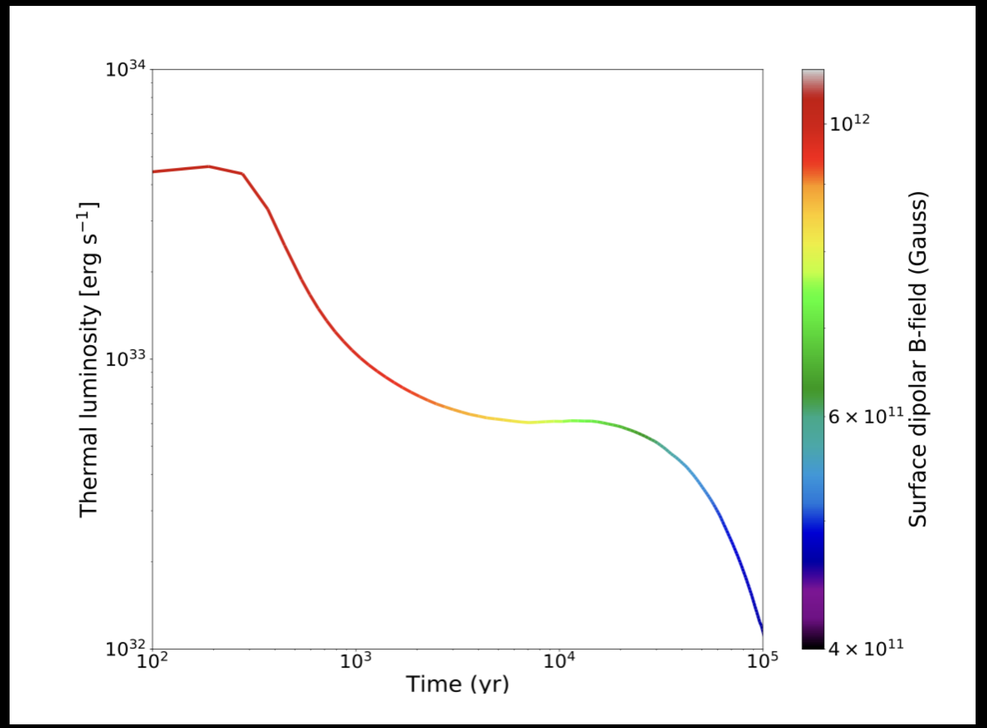

Core superconductivity

MHD-like approach

- Our model rely on Hall-Vinen-Bekharevich-Khalatnikov (HVBK) two-fluid model for describing superfluid/superconductor as a sum of a few fluids. We closely follow prescription developed by Glampedakis, Andersson & Samuelsson (2011) with simplifications by Graber, Andersson, Glampedakis & Lander (2015).

Single fluid system

$$\frac{\partial \vec{u}_c}{\partial t} = -\nabla \delta\mu_c + \frac{(\vec{\nabla} \times \vec{H}_{c1}) \times \vec{B}}{n_c} + \nu f(u_c)$$

$$\frac{\partial \vec{B}}{\partial t} = \vec{\nabla} \times (\vec{u}_l \times \vec{B}) + \frac{\vec{\nabla}^2 B}{\mathrm{Rm}}$$

$$\vec{\nabla} \cdot (n_c u_c) = 0 \qquad \vec{\nabla} \cdot (\vec{B}) = 0$$

$$\left.\frac{\partial B^l}{\partial r} + \frac{l+1}{r} B^l\right|_{r=R_{\mathrm{NS}}} = 0 \qquad J_r = 0$$

Stress-free boundary condition

$$\int \delta\mu_c \, dV = 0$$

u_l **is the vortex velocity**
Ohmic term is for numerical stability

Viscosity due to electron - electron scattering

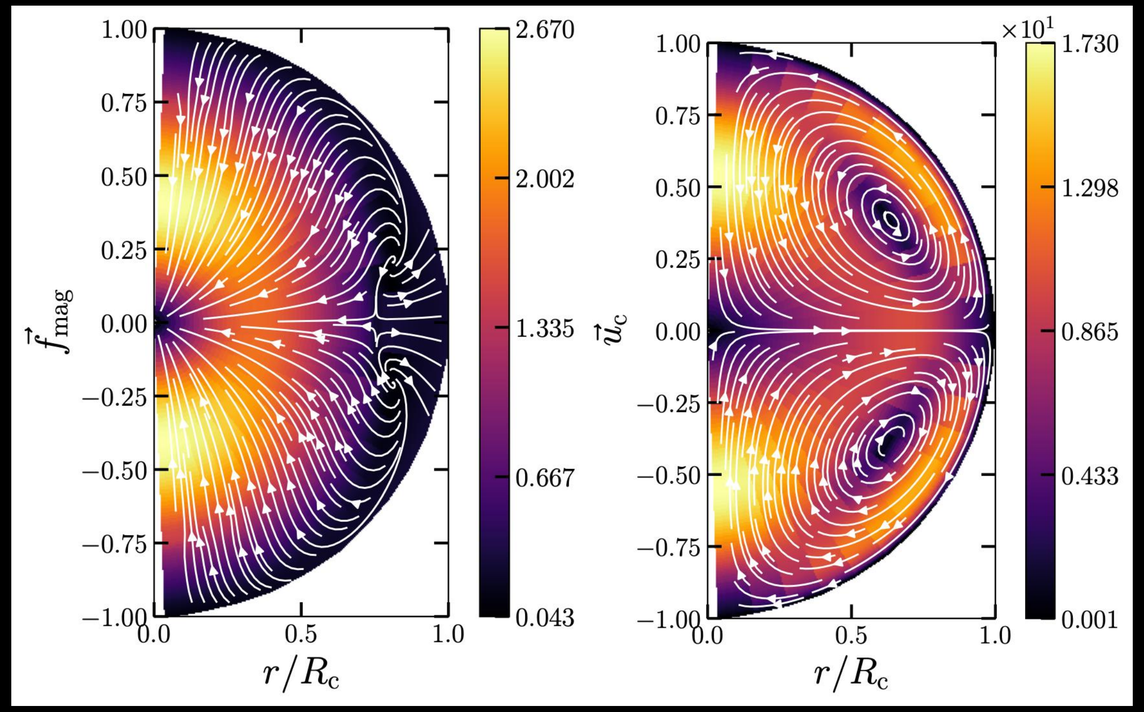

Boundary conditions

Vacuum

$$\frac{\partial B^l}{\partial r} + \frac{l+1}{r} B^l|_{r=R_{\mathrm{NS}}} = 0$$

Pseudo-vacuum

$$B_\phi = B_\theta = 0$$

Field lines approaches surface orthogonally

2D axial symmetry

Evolution towards stable configurations

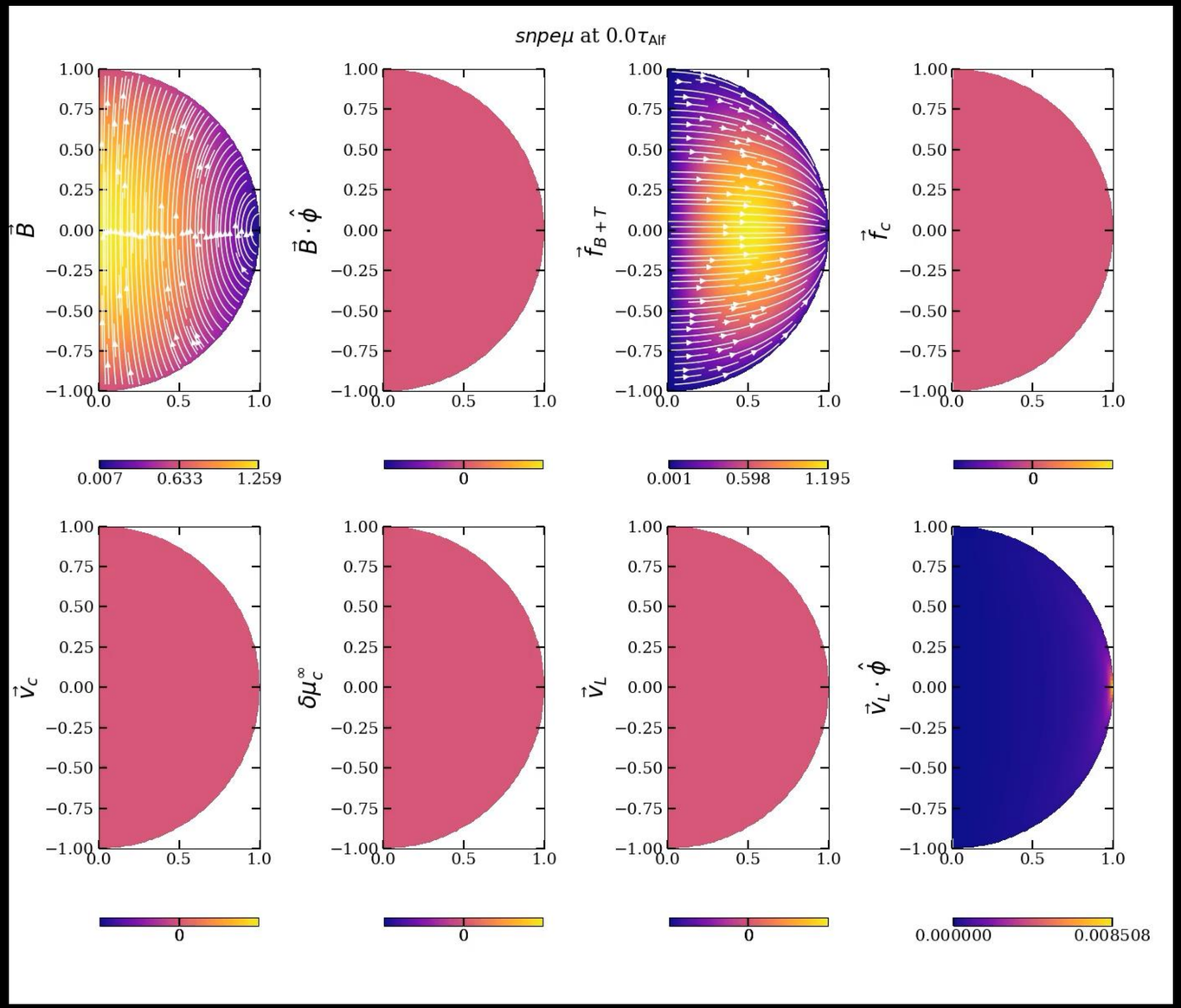

2D axial symmetry

Evolution towards stable configurations

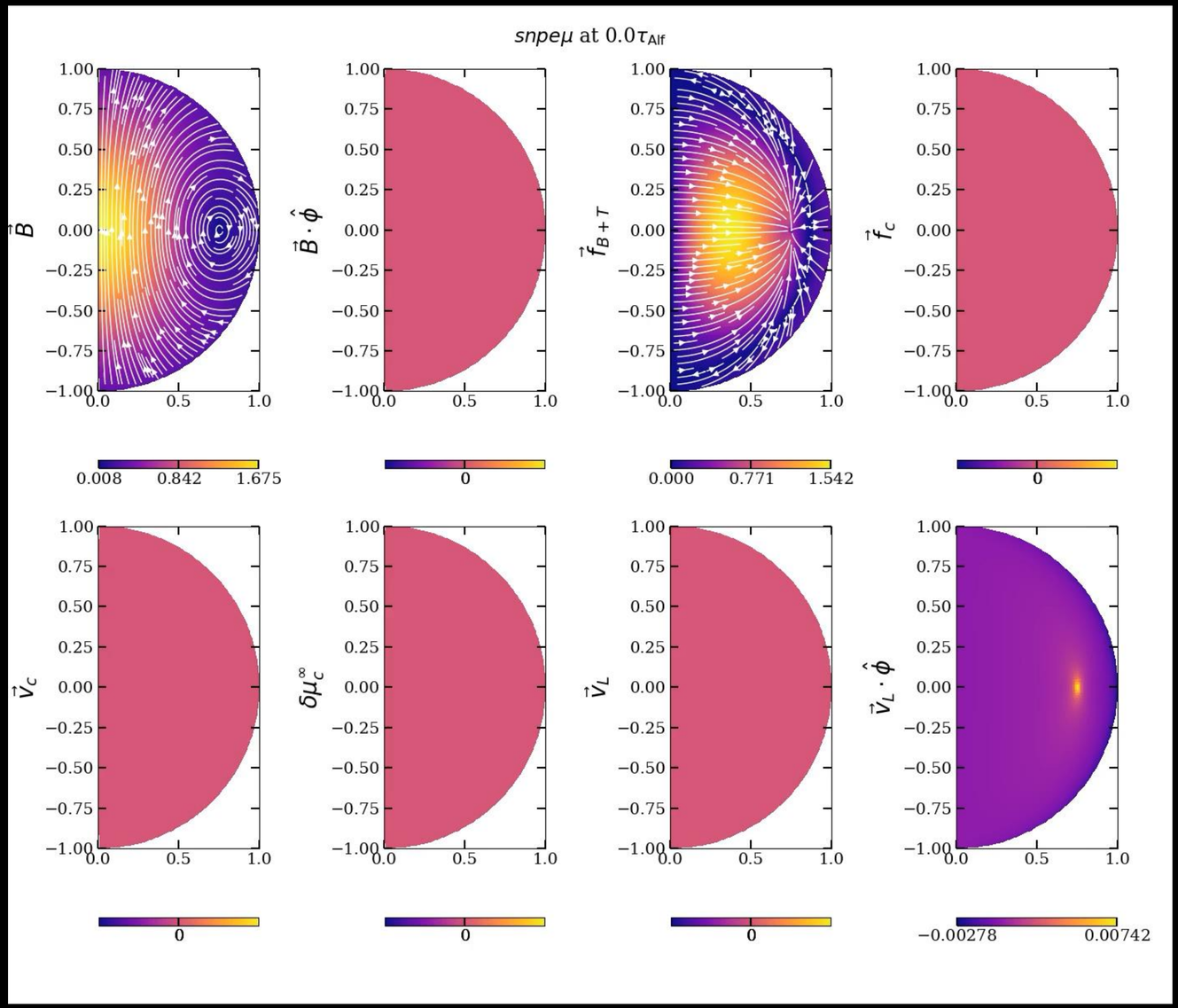

Energy evolution

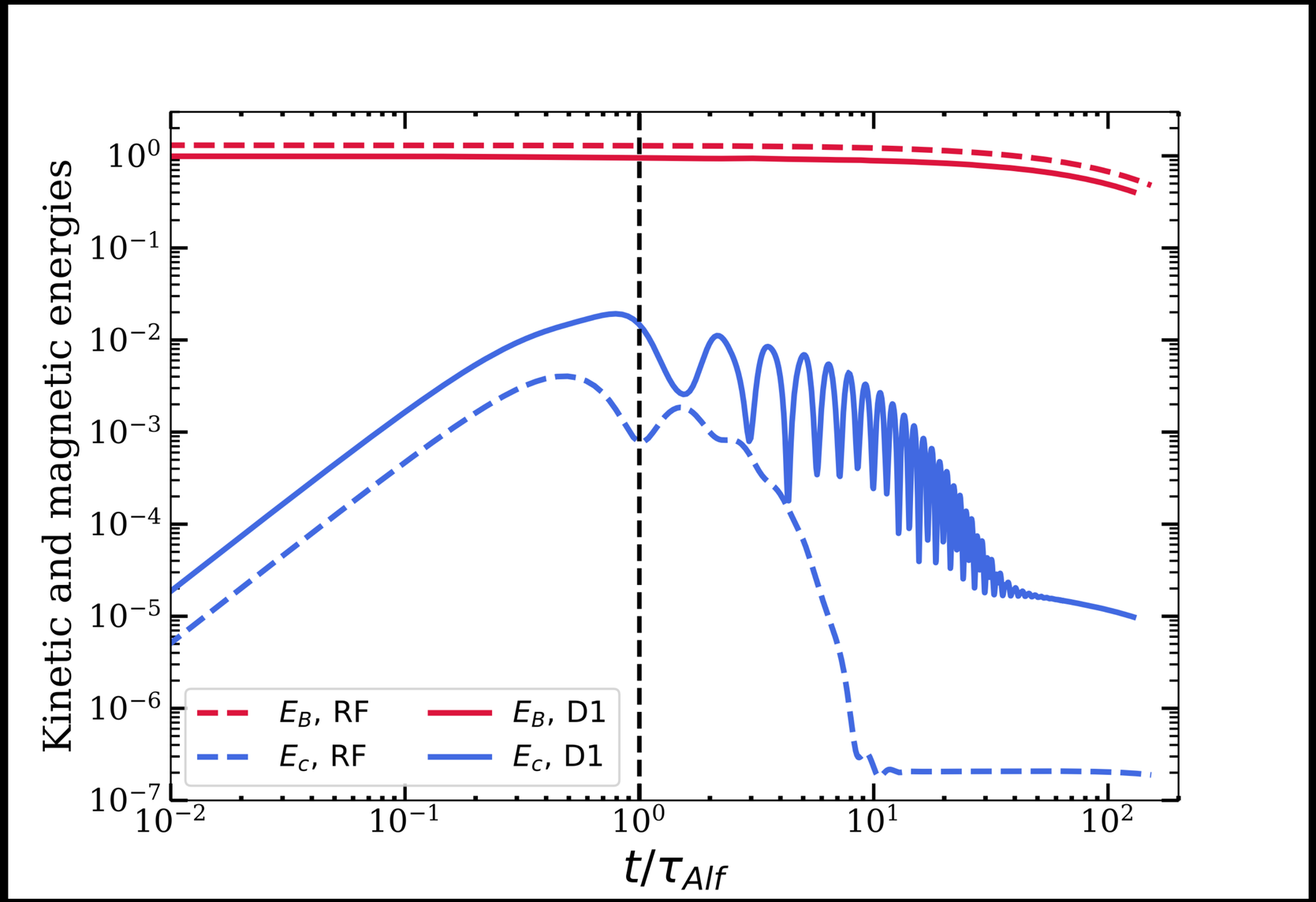

3D simulations

$v_l = v_c$

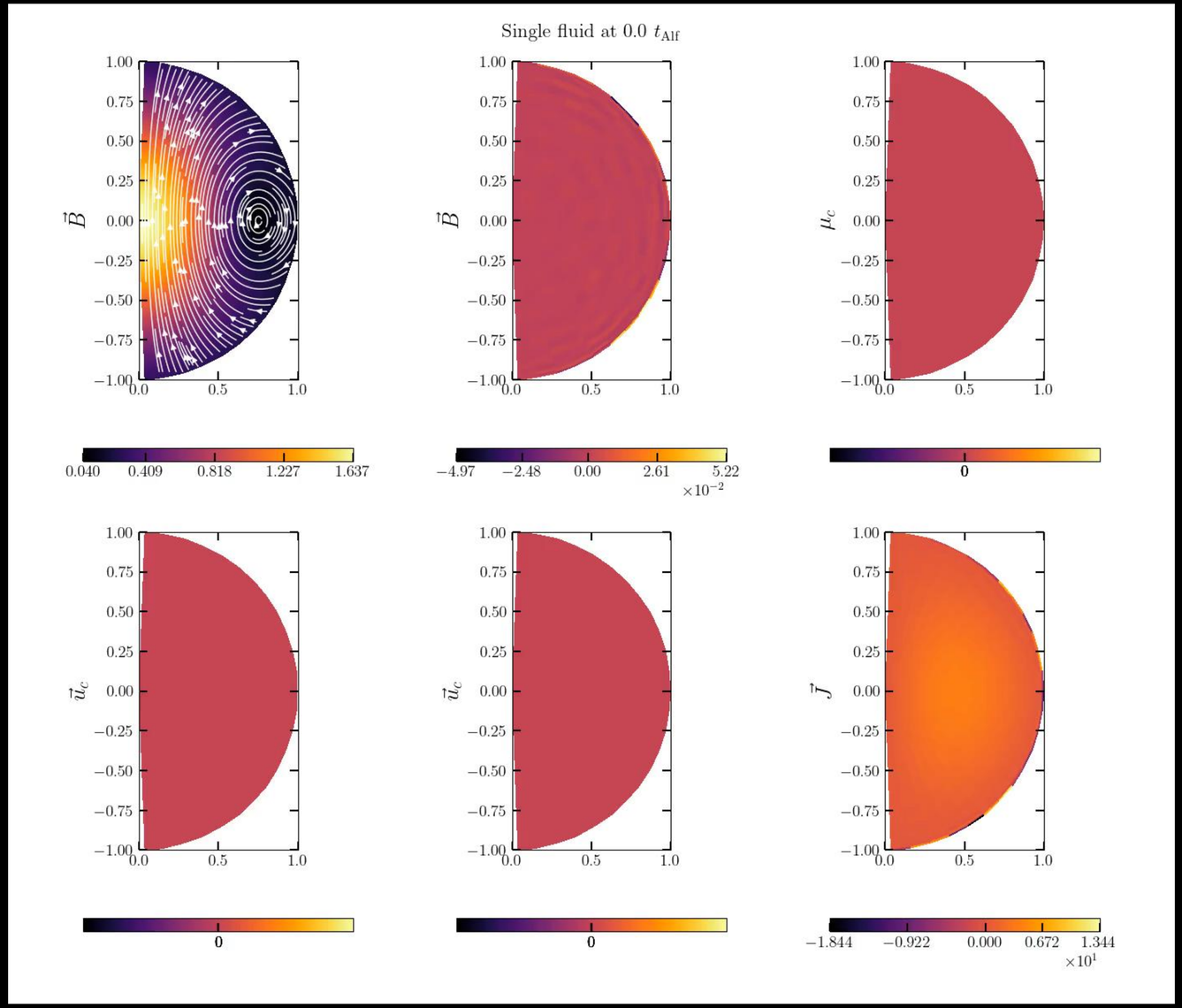

Summary and future work

- Magnetic fields of neutron stars are very complicated and might be the key to understand the NS diversity.
- Different types of neutron stars such as magnetars, XDINS, CCOs might be produced due to different type of dynamo mechanisms active at the proto-NS stage
- Convective dynamo combined with fast rotation might be responsible for classical magnetars; Tayler-Spruit for low-B magnetars and MRI for Central Compact Objects.
- Magnetic field evolution in the core is just started to be explored. Non-trivial interactions between the core and crust might lead to different energetic phenomena